Regulation of ion conductance and cAMP/cGMP concentration in megakaryocytes by light

***

Regulation der Ionenleitfähigkeit und cAMP/cGMP Konzentration in Megakaryozyten durch Licht

Doctoral thesis for a medical doctoral degree
at the Graduate School of Life Sciences,
Julius-Maximilians-Universität Würzburg,
Institute of Experimental Biomedicine I

submitted by

Hendrikje Kurz
from Berlin, Germany

Würzburg, 2020

Submitted on: …….

Office stamp

Members of the Thesis Committee:

Chairperson: **Prof. Dr. Wolfgang Kastenmüller**

Primary Supervisor: **Dr. Markus Bender**

Supervisor (Second): **Prof. Dr. Georg Nagel**

Supervisor (Third): **Prof. Dr. Alma Zernecke-Madsen**

Date of Public Defence:

Date of Receipt of Certificates:

Summary

Platelets play an essential role in haemostasis. Through granule secretion of *second wave* mediators and aggregation, they secure vascular integrity. Due to incorrect activation, platelet aggregation and subsequent thrombus formation can cause blood vessel occlusion, leading to ischemia. Patients with defects in platelet production have a low platelet count (thrombocytopenia), which can cause an increased bleeding risk. *In vitro* platelet generation is still in its development phase. So far, no convincing results have been obtained. For this reason, the health care system still depends on blood donors. Platelets are produced by bone marrow megakaryocytes (MKs), which extend long cytoplasmic protrusions, designated proplatelets, into sinusoidal blood vessels. Due to shear forces, platelets are then released into the bloodstream. The molecular mechanisms underlying platelet production are still not fully understood. However, a more detailed insight of this biological process is necessary to improve the *in vitro* generation of platelets and to optimise treatment regimens of patients.

Optogenetics is defined as “light-modulation of cellular activity or of animal behaviour by gene transfer of photo-sensitive proteins”. Optogenetics has had a big impact on neuroscience over the last decade. The use of channelrhodopsin 2 (ChR2), a light-sensitive cation channel, made it possible to stimulate neurons precisely and minimally invasive for the first time. Recent developments in the field of optogenetics intend to address a broader scope of cellular and molecular biology.

The aim of this thesis is to establish optogenetics in the field of MK research in order to precisely control and manipulate MK differentiation. An existing “optogenetic toolbox“ was used, which made it possible to light-modulate the cellular concentration of specific signalling molecules and ion conductance in MKs. Expression of the bacterial photoactivated adenylyl cyclase (bPAC) resulted in a significant increase in cAMP concentration after 5 minutes of illumination. Similarly, intracellular cGMP concentrations in MKs expressing photoactivated guanylyl cyclase (*Be*Cyclop) were elevated. Furthermore, proplatelet formation of MKs expressing the light-sensitive ion channels ChR2

and anion channelrhodopsin (ACR) was altered in a light-dependent manner. These results show that MK physiology can be modified by optogenetic approaches. This might help shed new light on the underlying mechanisms of thrombopoiesis.

Zusammenfassung

Thrombozyten sind für die primäre Hämostase verantwortlich und unterstützen die Blutgerinnung. Durch ihre Aggregation und die Synthese bzw. Freisetzung von in Granula gespeicherten *second wave* Mediatoren, sichern sie die Integrität der Blutgefäße. Werden Thrombozyten fälschlicherweise aktiviert, kann es zu einem Gefäßverschluss durch Thrombusbildung mit daraus resultierender Ischämie kommen. Patienten mit einer defekten Thrombozytopoese weisen eine reduzierte Thrombozytenzahl (Thrombozytopenie) auf, die mit einer erhöhten Blutungsneigung assoziiert ist. Bisher gibt es keine überzeugenden Ansätze, die eine Thrombozytenproduktion *in vitro* ermöglichen. Aus diesem Grund ist das Gesundheitswesen, in der Versorgung der bedürftigen Patienten mit Thrombozytenkonzentraten, auf Blutspender angewiesen. Thrombozyten werden im Knochenmark von ihren Vorläuferzellen, den Megakaryozyten (MKs) produziert. Diese bilden lange zytoplasmatische Fortsätze aus, die Proplättchen genannt werden. Durch die Scherkräfte des Blutstroms in den sinuosoidalen Blutgefäßen, schnüren sich Thrombozyten von den Proplättchen ab. Bisher sind die molekularen Prozesse der Thrombozytenproduktion noch weitgehend unverstanden. Ein besseres Verständnis des Vorgangs ist die Voraussetzung für eine Weiterentwicklung der *in vitro* Thrombozytengenerierung und einer optimierten Patientenbehandlung.

Unter Optogenetik versteht man die Übertragung lichtempfindlicher Proteine in zuvor nicht lichtempfindliche Zellen. Dadurch wird eine nicht-invasive Beeinflussung von Zellvorgängen oder des Verhaltens von Tieren durch Licht ermöglicht. Das Feld der Optogenetik, besonders der lichtempfindliche Kanal Channelrhodopsin 2 (ChR2), hatte einen großen Einfluss auf die neuronale Forschung. Durch ihn war es möglich, Neuronen gezielt nicht-invasiv zu aktivieren und Kreisläufe zu untersuchen. Mittlerweile wurde das Spektrum auf eine Vielzahl von Forschungsgebieten und Zelltypen ausgeweitet.

Das Ziel dieser Arbeit ist es, die Methoden der Optogenetik in MKs zu etablieren. Dadurch soll ein Weg gefunden werden, die Megakaryozytenreifung gezielt zu kontrollieren bzw. zu manipulieren. Die bereits vorhandene „optogenetische Toolbox“ wurde verwendet, um die intrazellulären Konzentrationen bestimmter Signalmoleküle und Ionen in MKs zu verändern. Durch die Expression der

bakteriellen fotoaktivierbaren Adenylatzyklase (bPAC), wurde die cAMP Konzentration nach 5 min Lichtgabe signifikant erhöht. Ebenfalls ist es durch die Expression der fotoaktivierbaren Guanylatzyklase (*Be*Cyclop) gelungen, die intrazelluläre cGMP Konzentration in MKs durch Belichtung zu erhöhen. Darüber hinaus konnte der Vorgang der Proplättchenformierung in MKs, welche die lichtempfindlichen Ionenkanäle ChR2 und Anion Channelrhodopsin (ACR) exprimierten, durch Licht beeinflusst werden. Die Ergebnisse zeigen, dass eine Beeinflussung der Megakaryozytenphysiologie durch Optogenetik möglich ist. Die Erkenntnisse können dazu beitragen, die Vorgänge der Thrombozytopoese in Zukunft besser zu verstehen.

Table of contents

1 Introduction

1.1 Megakaryocytes and platelets

1.1.1 From megakaryocytes to platelets

Haematopoietic stem cells (HSC) are the origin of all blood producing progenitor cells [1]. Haematopoiesis in adults is located mainly in the bone marrow (BM) [2]. In the embryonic phase HSCs are also present in the foetal liver, the spleen and the yolk sac [3, 4].

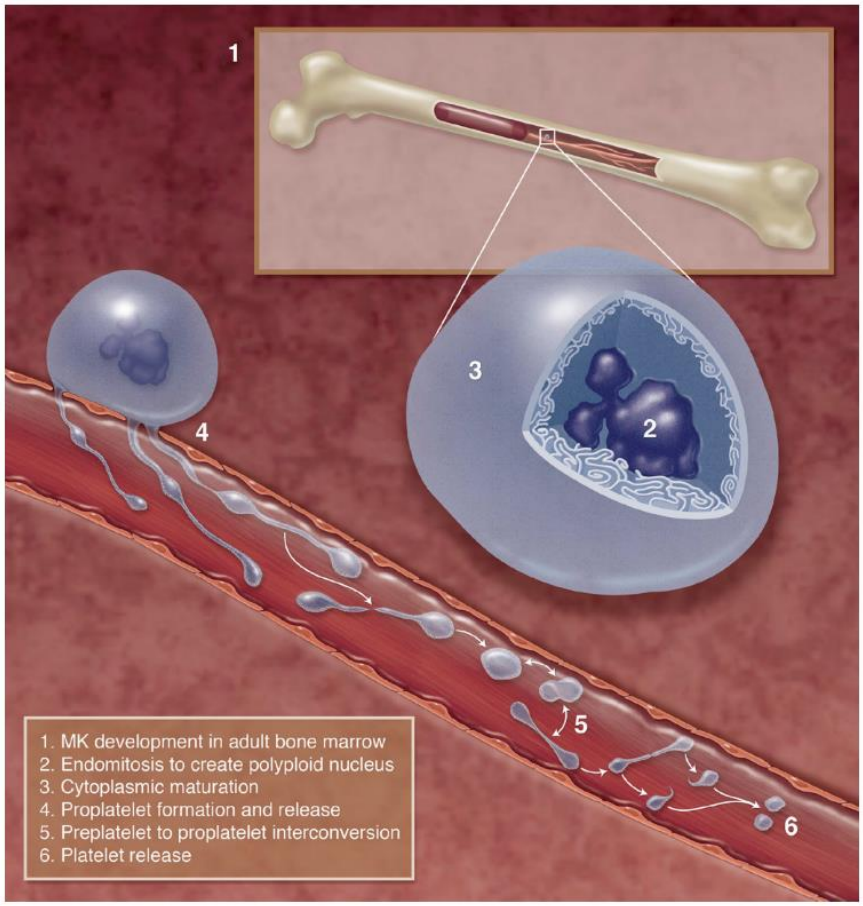

Figure 1: Megakaryocyte development and platelet release

Image taken from Machlus, K. R., & Italiano, J. E., Jr. (2013). The incredible journey: From megakaryocyte development to platelet formation. *Journal of Cell Biology*, 201(6), 785-796

In the trabecular structure of the BM, HSCs differentiate into megakaryocytes (MKs). MKs only represent 0.05% of all nucleated cells in the BM [5]. They have an average size of 50-100 µm and can produce up to 5000 platelets each [3, 6]. Before having the ability to release platelets, MKs undergo a complex process of differentiation. The decisive factors which trigger MK maturation and initiate proplatelet formation are still largely unknown. Through interactions of MKs with osteoblasts and binding of thrombopoietin (TPO), collagens and pro-inflammatory cytokines, their maturation is supported while proplatelet formation is still suppressed [7-10]. The sinusoidal network of the BM is lined with discontinuous endothelium [11, 12]. The endothelium releases cytokines and adhesion molecules which are important for the mobilisation and orientation of MKs [13]. At the beginning of the maturation process, MKs multiply their DNA without cell division. This procedure is called endomitosis. Due to this, MKs can reach a ploidy of 128n [6]. Thereby, the nucleus develops a multilobulated shape and the cytoplasm expands [14]. After endomitosis completion, an invaginated demarcation membrane system (DMS) is established which provides the resources for future platelet membranes. During this process, the DMS stays in contact with the plasma membrane [15-17]. Platelet specific proteins are then synthesised and packed into granules [3]. Via chemotaxis mature MKs are guided to the BM sinusoids [18]. When the MKs reach the vessels, they can form cytoplasmatic protrusions, called proplatelets, through the discontinuous endothelium into the sinusoids of the BM. Due to shear forces, they release platelets and platelet-like fragments into the blood stream [19, 20]. The remaining nucleus is extruded and degraded [15].

β1-tubulin is the most important tubulin in MKs. It has a significant influence on proplatelet formation. In the early maturation process, microtubules are oriented radially, originating from the nucleus. Beginning at one pole, MKs extend pseudopodia which thin out towards the periphery [14]. The microtubules arrange in bundles and follow the extensions [21]. Dynein, a motor protein, is responsible for the elongation process of the protrusions. It enables the microtubules to slide against each other and thus, extending the proplatelets. They can extend, stop during the elongation process or retract [3, 20]. At the tip of the protrusion, the microtubule bundles bend and turn back towards the cell body. F-actin, which is

present in the entire proplatelet, is responsible for the branching process. Together with myosin, F-actin bends the microtubule bundles. As platelets are only released at the end of a proplatelet, multiple branches are formed to increase the number of ending points [21].

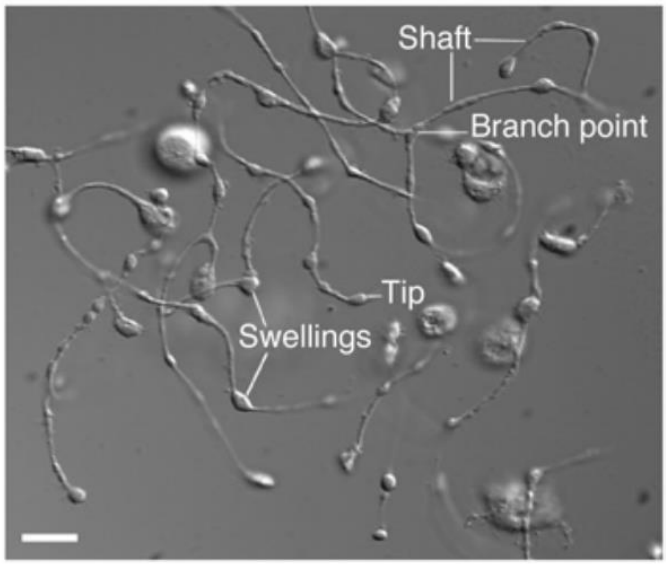

Figure 2: Anatomy of a proplatelet

Representative image of a proplatelet forming MK *in vitro*. Scale bar 5 µm

Image taken from Patel, S. R., Hartwig, J.H. & Italiano, J. E., Jr. (2005). The biogenesis of platelets from megakaryocyte proplatelets. *Journal of Clinical Investigations*, 115(12), 3348-3354

Platelet granules and organelles are transported to the proplatelet tips along microtubules via kinesin. When all components are present, the proplatelet pinches off the platelet [9, 19, 22]. The diameter and thickness of the marginal band, consisting of multiple microtubules, determines the size of the released fragments [23]. As in the elongation process, the release of platelets is probably also driven by microtubule sliding [20]. Aside from platelets, larger fragments, termed preplatelets, are released into the blood stream. Preplatelets vary in size of 2-10 µm and are anucleate. They usually have a dumbbell-like shape and can release further platelets [24]. The release of platelets and platelet-like fragments can be visualised via two-photon-intravitalmicroscopy in mice [25].

1.1.2 Aspects of platelet function

150-400x10^9/l blood platelets circulate through the human body. On average they are exchanged every 10 days [26]. Platelets have a size of 2-3 µm, no nucleus and a discoid shape [27]. One of their main functions is primary haemostasis.

The cytoskeleton of platelets is formed by tubulin and actin polymers. Different isoforms of tubulin polymers, called *alpha*- and *beta*-tubulin, combine to form so called microtubules. The microtubules are the basic structure of discoid shaped platelets. At one microtubule end (+ end), molecules can attach and at the other end (- end), they dissociate. This allows a quick and flexible adjustment of the shape. The majority of actin is organised in filaments which reinforces the scaffold. The other part is bound in complexes, so that molecules cannot bind uncontrolled to the filaments. Additionally, the filament ends are occupied by molecules to prevent an accumulation. When platelets are activated, the molecules at the ends are released, and the actin filaments can reorganise themselves [19].

Platelets contain at least three major types of granules. *Alpha*-granules incorporate adhesion molecules (fibrinogen, von-Willebrand-Factor (vWF)) and cytokines. Adenosine diphosphate (ADP), serotonin and histamine can be found in dense granules. Lysosomes are filled with proteolytic proteins [28, 29]. Platelets are activated after contact with damaged endothelium. On the therefore exposed collagen, plasma vWF is immobilised [30]. Numerous receptors are present on the platelet surface. This includes glycoprotein (GP) receptor Ib which binds to the collagen-immobilised vWF. Via interaction with the GPIb-V-IX-receptor complex, the reversible attachment of platelets to the vessel wall is enabled. However, this interaction is only transient. Therefore, GPVI binds to exposed collagen and activates further platelets and thereby stabilises the binding and activates the platelets [31, 32].

Integrins are “two-faced” receptors. The extracellular part interacts with the extracellular matrix and the intracellular part transduces the signals into the cell. When surface receptors bind to ligands, the integrins change from a low-affinity to a high-affinity state. This process is called “inside-out” signalling and is mediated via G-protein-coupled receptors (GPCR) and the immunoreceptor

tyrosine-based activation motif (ITAM) pathway [33-36]. Platelets synthesise and release further mediator substances like thromboxane A2 or ADP of their granules, respectively [37]. The binding of ligands, such as fibrinogen, to the αIIbβ3-receptor initiates an “outside-in” signalling. This includes multiple intracellular signalling cascades, which result in a reorganisation of the cytoskeleton leading to a shape change of the platelet from a discoid to a spherical form [38-40]. Platelet aggregation and conformational changes enable the formation of a cluster, which covers the initial endothelium defect [41].

Besides their function in haemostasis, platelets are involved in other processes in the body. By releasing growth factors, platelets have a positive influence on wound healing and tissue regeneration [42]. Other platelet factors can promote or prevent angiogenesis. It was demonstrated that proteins, which support angiogenesis, are stored in different *alpha*-granules compared to the ones which suppress the formation of new blood vessels. Thus, a targeted effect of platelets is possible [43]. Moreover, platelets can influence the spreading of cancer cells. Malignant cells can activate platelets and can therefore adhere more easily to vessel walls [44]. Platelets might even form a protective wall around malignant cells to shield them from degradation by natural killer cells [45].

1.1.3 Apoptosis in MKs and platelets

Apoptosis is a necessary biological process and can be triggered by various stimuli. It is important for cell regeneration, disposal of damaged cells or the natural limitation of cell count. There are two different pathways which lead to apoptosis, the intrinsic and the extrinsic pathway [46]. Normally, proapoptotic and prosurvival factors in a cell are in equilibrium. If the balance is shifted towards proapoptotic factors, e.g. in the event of DNA damage, the intrinsic pathway is initiated [47]. The activity of proapoptotic factors induces the permeability of the outer mitochondrial membrane, thereby releasing harmful factors (e.g. cytochrome c) into the cytosol. These factors trigger the caspase cascade [48]. Caspases (*c*ysteinyl *asp*artate protein*ases*) are involved significantly in the process of cell death [49]. The cascade of the intrinsic pathway starts with initiator caspase 9 which activates the effector caspases 3, 6 and 7 [46]. As a result, the mitochondrial potential is destructed. The extrinsic pathway is initiated by the

binding of ligands (e.g. TNF-α, FAS) to the extracellular death receptors [48, 49], thereby activating the initiator caspase 8 which in turn activates the effector caspases 3, 6 and 7 [46]. Additionally, caspases have an influence on the phosphatidylserine exposure. This protein is transported to the cellular membrane and is a signal for the degradation of the cell. Caspases inactivate flippases, which normally transport phosphatidylserine ATP-dependent from the outer to the inner membrane leaflet, and activate scramblases, which can transport proteins ATP-independently between the leaflets of the bilayer membrane. Due to the phosphatidylserine exposure, the cell is phagocytised [50, 51].

Platelets *in vitro* can show typical signs of apoptosis, like loss of mitochondrial potential, increased permeability of the mitochondrial outer membrane, phosphatidylserine exposure and caspase activity [52, 53]. In platelets, phosphatidylserine exposure can be triggered either by apoptosis [52] or after agonist activation [54, 55]. However, phosphatidylserine exposure after agonist activation is calcium-dependent whereas in case of apoptosis it is calcium-independent [48, 50].

1.1.4 Influence of ion influx and intracellular ion concentrations on MK metabolism and platelet behaviour

Ion channels transport charged particles across membranes. Changes in the intracellular ion concentration can influence cell size and volume as well as membrane potential [56, 57]. Different methods can be used to investigate the expression and function of ion channels in cell membranes, for instance the patch clamp method. It allows the recording of electrophysiological events [58]. It is a major challenge to study the properties of the platelet plasma membrane using the patch clamp technique, due to the small size of platelets. Therefore, MKs, as platelet progenitors, are a valuable tool to investigate ion channels in the cell membrane and how they contribute to cell homeostasis [59]. Possible results can give indications for the role of ion channels in platelet membranes. Furthermore, genetic modified mice enable investigators to study possible consequences of modified ion channels on platelet function.

Various ions have an influence on MK homeostasis and platelet behaviour. Important ions in this context are zinc, potassium, magnesium and calcium.

Zinc is a ubiquitously occurring cofactor of proteins and enzymes. In its role as second messenger, zinc may contribute to various signal pathways in platelet homeostasis and support platelet activation through agonists or rather it acts as agonist itself [60-62]. In MKs, zinc ions may contribute to proplatelet formation and development of *alpha*-granules [63].

Analysis of depolarisation-gated K^+-selective (Kv) channels in MKs and platelets identified the Kv1.3 subunit as the relevant component of these channels. The data points to a contribution of the conducted K^+ in maintaining the membrane potential and the number of generated platelets [64].

It was revealed that the transient receptor potential melastatin-like 7 (TRPM) channel is a Mg^{2+} transporting channel. Platelet- and MK-specific TRPM7 knockout mice displayed macrothrombocytopenia. The dysfunctional proplatelet formation might be due to enhanced microtubule assembly [65]. Therefore, magnesium seems to be crucial for a normally functioning cytoskeleton and proplatelet formation.

Calcium is an important second messenger in platelet homeostasis. It is involved in granule secretion, as well as reorganisation of the cytoskeleton which causes platelet shape change. Furthermore, calcium contributes to platelet aggregation [36, 66, 67]. The most important calcium channels for platelet function are P2X1 channels, Orai1 and IP3R (inositol 1,4,5-triphosphate receptor) channels [57]. P2X1 channels are selective cation channels which are activated by adenosine triphosphate (ATP). After cells are damaged, they release ATP. Thereupon, P2X1 receptors are activated and mediate a fast calcium influx into platelets [57, 67]. Orai1 is the central pore of the calcium release activated calcium (CRAC) channel [68, 69]. This channel has a high conductance for calcium ions and is activated by stromal interaction molecule 1 (STIM1). STIM1 is a sensor which is located in the dense tubular network, the intracellular calcium storage in platelets. If the calcium concentration falls below a certain value, STIM1 opens Orai1 channels in the plasma membrane, a process termed store-operated calcium entry (SOCE), which in turn allows calcium influx [57, 70-73]. A

point mutation in the STIM1 EF binding motif results in impaired calcium binding in the dense tubular network and permanently opens calcium channels in the plasma membrane. Mice with point mutated STIM1 show macrothrombocytopenia and an increased intracellular calcium concentration, leading to preactivated platelets and a reduced platelet count, due to rapid platelet clearance from the circulation. However, MK differentiation and proplatelet formation are unaltered [74]. Mice deficient in Orai1 or STIM1 display normal megakaryopoiesis and platelet production, but loss of one of the two proteins reduces the ability of platelets to form thrombi under high shear forces *in vivo* and *in vitro*, whereas the bleeding time is only slightly prolonged. Additionally, GPVI-mediated platelet activation through collagen, CRP or convulxin is impaired [75]. Orai1 might be a potential starting point for a new antithrombotic therapy. It has been demonstrated that the channel is essential for platelet aggregation and first data indicates that antagonization of the channel reduces arterial thrombus formation [76, 77]. IP3R channels are non-selective cation channels in the dense tubular network. They are activated by calcium and inositol triphosphate (IP3). Their significance in MKs is still unknown [80-82].

Interestingly, Di Buduo and colleagues could unveil the role of Ca^{2+} compartmentalisation in regulating different MK functions. Ca^{2+} mobilisation from intracellular stores was important for MK adhesion and proplatelet formation, while extracellular Ca^{2+} entry following store depletion is primarily responsible for promoting cytoskeletal reorganisation and subsequent migration on extracellular matrix (ECM) components (through myosin light chain-mediated remodelling of actomyosin cytoskeleton) [78]. Furthermore, it was shown that c-Mpl downstream signalling activation is sustained by Ca^{2+} mobilisation, which has an impact on MK proliferation [79].

In conclusion, ions play an important role in MK and platelet homeostasis. Many ion channels in MKs and platelets, especially those specialised in calcium transport, have been identified. However, their precise function needs to be further explored [57].

1.1.5 Platelet production *in vitro* – Where do we stand?

A reduced platelet count (<150.000/µl), is referred to as thrombocytopenia. In most cases, this is due to an impaired thrombopoiesis or an increased platelet clearance [27, 83]. If it is an issue of chronic thrombocytopenia or slowly decreasing platelet count, the body can adapt to the new situation and the effects of the reduced platelet count might not be as obvious. Nevertheless, it might lead to an impaired haemostatic function and bleeding diathesis. The most common treatment of a severely reduced platelet count is platelet transfusion. According to the current state of knowledge, it is not yet possible to generate platelets in adequate numbers *in vitro*. Because of that, the medical sector still relies on healthy blood donors [6]. The storage of platelet concentrates is cumbersome and expensive. In general, they can only be kept for about 5 days, before the risk of bacterial contamination increases and the functionality of the cells is reduced [84, 85].

In order to find an alternative to platelet donation, thrombopoiesis needs to be examined more closely. The cultivation of MKs is very complex, and the BM environment is difficult to mimic *in vitro*. Previous research identified important factors. First, it was shown that MKs release more platelets if they are exposed to shear forces [86]. And secondly, TPO was determined to be the significant factor of MK maturation [87]. For many years, the importance of TPO was only suspected. In 1994, different groups described their findings on TPO independently of one another [88-91]. The discovery of TPO as a substantial factor for MK development was a scientific breakthrough [8, 92]. With the opportunity to supplement cell cultures with TPO, it became possible to study MK maturation *in vitro*. TPO interacts with the MK specific c-Mpl-receptor and activates transcription factors [93, 94]. The factor affects the ploidy and size of MKs as well as the expression of surface receptors on MKs [95]. At low platelet count, TPO concentration increases due to a positive feedback mechanism [93].

In most experimental approaches, CD34 positive HSCs are used for the cultivation of platelets *in vitro*. HSCs are obtained from umbilical cord blood, peripheral blood or the BM [6]. Matsunaga *et al.* developed a three-phased culture system, which enables the generation of platelets from human cord blood

HSCs. Their functionality is described to be comparable to *in vivo* platelets [96]. Further experimental approaches used induced pluripotent stem cells (iPSCs). This cell type has an advantage of an almost endless capability for cell division, without loss of product quality. They can also be easily genetically modified. Some diseases and medication tests are falsified or not feasible in animal models. In these specific cases iPSCs can be a benefit. They provide a model with almost human-like conditions [97]. A major problem of blood transfusions is the production of antibodies in reaction to foreign blood cells. iPSCs could be a possible approach to customise blood products without incompatibilities [97]. The disadvantage of iPSC cultures is the considerable additional time needed. Studies have shown that iPSCs first release platelets into the culture only after 22-26 days [6, 98]. Furthermore, the yield of platelets is rather low.

Meanwhile, there are attempts to reproduce the BM structure in a three-dimensional culture. One example is a woven polyester surgical fabric scaffold in a 3D single pass perfusion bioreactor system. Compared to a two-dimensional culture, the cord blood culture in the bioreactor produced more platelets [99]. Another example is a 3D network out of silk tubes which represents the small vessels of the BM [100]. A further possibility to study MK differentiation in the BM is a bone marrow-on-a-chip. There are different bone marrow-on-a-chip models. For example, a specialised tube imitating the BM structure is implanted subcutaneously for 4-8 weeks. During this time, the inner tube enriches with BM cells. After explantation, the bone marrow-on-a-chip is applied to a flow chamber and supplied with nutrients. This model is able to mimic the BM microenvironment [101]. Another variation of the bone marrow-on-a-chip is a platelet bioreactor-on-a-chip consisting of two channels that simulate vessels as well. Columns between the channels form pores, modelling the discontinuous endothelium of the sinusoids. The channels are coated with ECM proteins. By infusing MKs into the upper channel and applying continuous flow, Thon *et al.* managed to induce proplatelet formation through the pores into the lower channel and produced platelets [102]. With the different bone marrow-on-a-chip models it is possible to investigate the effects of radiation or specific medication on the BM [101].

So far, no approach was able to provide enough platelets for medical use. Additionally, the functionality of the generated platelets *in vivo* is uncertain. Until now, it is insufficiently known which triggers initiate proplatelet formation. Thus, this needs to be further examined. Nevertheless, new opportunities may arise which could lead to more individual therapeutic options and an improved treatment for patients [6].

1.2 Relevance of cAMP, cGMP and phosphodiesterases

Cyclic adenosine monophosphate (cAMP) is an important second messenger, which is involved in many cell processes, e.g. glycogenolysis and lipolysis [103]. The cAMP-dependent kinase, protein kinase A (PKA), is part of the cAMP signal pathway and phosphorylates different molecules. Among others, DNA-expression of transcription factors and the opening state of an ion channel can be modified by the binding of cAMP [104]. The second messenger is generated by an activated adenylyl cyclase. Each organism has different stimuli for the production of cAMP, e.g. lack of glucose in prokaryotes or lack of CO_2 in eukaryotes and bacteria [105, 106]. Adenylyl cyclases have the greatest influence on intracellular cAMP concentration [104].

Guanylyl cyclases are related to sensor proteins. They can transfer information via cyclic guanosine monophosphate (cGMP) to other molecules, which can thereby activate or inhibit signalling pathways. The second messenger cGMP can activate protein kinase G (PKG) or CNG (cyclic-nucleotide gated) channels. It is involved in various processes e.g. the relaxation of smooth musculature, sperm motility or the visual process in animals [107, 108].

cAMP and cGMP content is dependent on the interplay between adenylyl- /guanylyl cyclases and phosphodiesterases (PDEs). On one hand the second messengers are synthesised by the cyclases and on the other hand they are hydrolysed by PDEs [109]. The enzyme group of PDEs is divided up into 11 families [110]. Three different types of PDEs (PDE 2A, 3A, 5A) are detected in platelets [111]. They may also be found in MKs as platelet progenitors. Begonja *et al.* investigated the significance of cAMP and cGMP as well as the expression of PDEs in MKs. They demonstrated, that PDE3 A and PDE 5 content

increased during MK differentiation [112]. The interplay between different PDEs is rather complex. The effects on the second messenger concentrations cannot be clearly attributed to one specific PDE subtype. Most PDEs are able to hydrolyse both, cAMP and cGMP. However, they differ in their efficiency and specificity. PDE 2 hydrolyses cAMP and cGMP equally. A high concentration of cGMP increases its activity. That means, cGMP supports the degradation of cAMP [111, 113]. PDE 3 can degrade cAMP and cGMP. Despite similar binding affinity, the hydrolysation of cAMP predominates because this process is more efficient. Additionally, PDE 3 is inhibited through cGMP, which is why it is called cGMP-inhibited PDE [114, 115]. PDE 5, rather specifically, hydrolyses cGMP. The binding affinity for cGMP is 100-fold higher than for cAMP. By binding cGMP, PDE 5 is able to increase its activity [110, 111]. In summary, cGMP may support the degradation of cAMP through the induction of PDE 2 and it may also prevent the degradation of cAMP by simultaneously inhibiting PDE 3 [111, 113].

Table 1: Characteristics of PDEs

Type	**Specificity**	**Characteristics**
PDE 2	cAMP = cGMP	cGMP induces PDE activity
PDE 3	cAMP > cGMP	cGMP inhibits PDE activity
PDE 5	cAMP < cGMP	Binding affinity for cGMP is 100x higher than for cAMP

Adapted from Bender, A. T., & Beavo, J. A. (2006). Cyclic nucleotide phosphodiesterases: molecular regulation to clinical use. *Pharmacological Reviews*, 58(3), 488-520

Inhibitors can be used to reduce the activity of PDEs and in consequence increase the second messenger content. In the experiments conducted in this study, the PDE 3 inhibitor cilostazol and the PDE 5 inhibitor dipyridamole were used. The chemicals were chosen because these particular PDE subtypes have strong influence on the degradation of second messengers in platelets [116]. Cilostazol is a PDE 3 inhibitor and increases the cAMP concentration by inhibiting its degradation. The chemical might even inhibit cGMP hydrolysis through PDE 5.

Furthermore, cilostazol suppresses the uptake of adenosine and therefore increases the extracellular adenosine concentration. This can lead to an cAMP increase in platelets, among others [109, 117]. Dipyridamole inhibits PDE 5 and therefore increases the cGMP concentration. Additionally, it induces prostacyclin synthesis and suppresses adenosine uptake [114, 118, 119].

The influence of second messengers during MK maturation is not well understood. First results indicate that the second messengers cAMP and cGMP play an important role during this process. cAMP levels and the protein expression of the cAMP signalling pathway increase during MK maturation. cGMP levels rise during the early maturation period but decrease again quickly. This might be due to high expression of PDE 5 in mature MKs. Both second messengers might have an influence on the MK actin cytoskeleton. This is because high levels of cAMP inhibit, whereas high levels of cGMP support proplatelet formation [112]. These findings indicate that cAMP is a possible starting point to manipulate MK maturation.

1.3 Optogenetics

1.3.1 Overview

Optogenetics is a method to specifically influence cells or freely moving organisms in a non-invasive way by light [120]. This is possible due to the “introduction of light-sensitive proteins into otherwise light-insensitive cells” [121]. Some key aspects of this rather new field of science have been known for a long time but have been studied only in recent years [120].

Stoeckenius and Oesterhelt laid the foundations with the discovery of bacteriorhodopsin (BR) in 1971. This protein complex was detected in the purple membrane of *Halobacterium salinarum* and appeared to be a photoreceptor because of great similarities to known rhodopsins. Until then, retinal-protein complexes were only known in animals [122]. It was later discovered that BR functions as a light-sensitive proton pump [123]. The ion transport across the membrane causes hyperpolarisation [124]. Because of its characteristics as a stable membrane protein as well as its easy extraction in great quantities, BR

became a model protein in the following years. BR has been used to study ion transport and light-energy conversion [125]. There have been indications that suggest *Halobacterium salinarum* to contain more than two light-sensitive proteins [126]. A few years later, the spectrum was expanded with the discovery of halorhodopsin (HR). It was also detected in *Halobacterium salinarum* [127]. This protein is a light-activated chloride pump that is triggered by yellow light (580 nm) [128, 129]. HR enables the organism to maintain homeostasis in an environment with a high salinity which is achieved by the transport of chloride ions into the cell [130]. However, the main drawback of these ion pumps is that they can only transport one ion per photocycle [131].

The following discovered proteins were called sensory rhodopsin 1 and 2. As phototactic receptors [132], they help the organism to find ideal light conditions in which the ion pumps (BR and HR) can work effectively. Additionally, harmful UV-light is avoided. Due to phototactic and photophobic effects, the swimming behaviour of *Halobacteria* is affected [133]. The sensory information is transferred into a protein-interaction network via halobacterial transducer (Htr) [134].

A breakthrough in the field of optogenetics was the discovery of channelrhodopsin (ChR) [135]. ChRs combine both the light sensor and the ion channel into one protein complex [136, 137]. After stimulation with blue light, a passive cation flow is generated across the cell membrane. The cation flow is independent of the photocycle [138]. It was demonstrated that the non-selective cation transport causes depolarisation of the membrane of human cells [125]. ChR was established in various cell types by different working groups. For instance, the expression of the light-sensitive channel in the muscle cells of *Caenorhabditis elegans* led to contractions of the nematode after illumination [139]. A specific depolarisation was triggered in rat neurons [140]. Another working group expressed ChR in the inner retinal neurons of mice. They were blind, due to a photo degenerative disease (e.g. retinitis pigmentosa). The light-sensitive channel transformed the inner retinal neurons into photo-sensitive cells. Because of this, these mice were able to sense light signals again and transferred the information to their visual cortex [141]. These applications provide the basis for what we call “optogenetics” today [125].

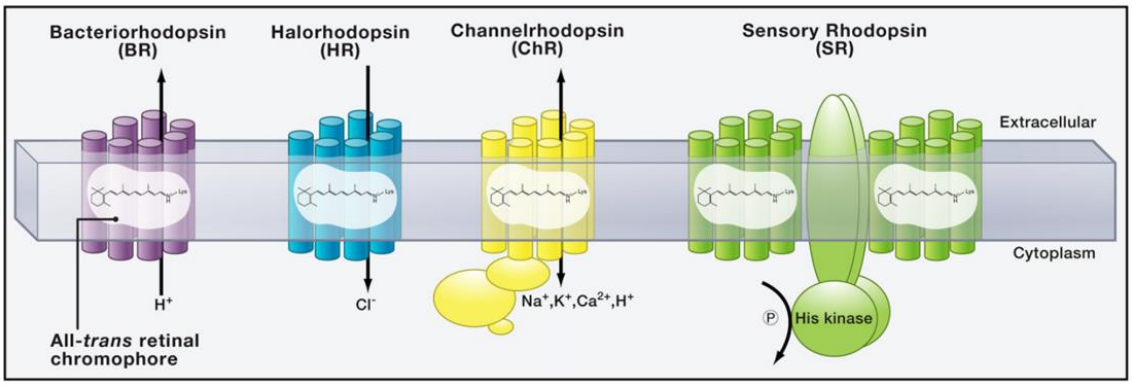

Figure 3: Microbial rhodopsins Type I

BR pumps protons from the cytoplasm into the extracellular space; HR pumps chloride into the cytoplasm; ChR transports cations across the membrane bidirectionally but always along the electrochemical gradient of the transported ion; SRs lack transmembrane ion transport in the presence of His kinase transducer protein Htr

Image and description taken from Zhang, F., Vierock, J., Yizhar, O., Fenno, L. E., Tsunoda, S., Kianianmomeni, A., {…}, Deisseroth, K. (2011). The microbial opsin family of optogenetic tools. *Cell*, 147(7), 1446-1457.

New opportunities are being developed, especially in the field of neurobiological research. To learn more about neuronal connections and the impact of neurological diseases, the neuronal activity needs to be controlled, for instance via light which can be used to switch neurons on and off [129]. So far, scientists have been using electrodes for the stimulation of neurons, which is imprecise, as cells cannot be stimulated at the same time. In particular, the research on free moving animals is limited, due to technical restrictions. Based on the new findings in the field of optogenetics it is possible to have “minimal{ly} invasive, genetically targeted and temporally precise control of neural activity” [121].

Meanwhile, there is a fibreoptic system, termed optical neural interface - ONI, which makes it possible to send light to deeper brain structures of a living animal. For this purpose, a lead structure is implanted into the skull of an animal. This serves as access for the virus, which transfers the optogenetic construct into neurons, as well as for an optical fibre. This fibre is connected to a laser and has a diameter of only 200 µm. This enables the precise stimulation of neurons of freely moving animals [142].

Additionally, transgenic mouse lines, which express ChR2, have been generated and enable scientists to study neural circuits *in vivo* [143].

Furthermore, existing constructs have been modified and improved. There are approaches to combine contrary constructs and establish them into one organism, such as ChR (cation channel/depolarisation) and HR (chloride pump/hyperpolarisation). The light spectra which activate the respective construct differ more than 100 nm from each other. This makes it possible to activate the constructs separately [130, 144].

Optogenetics offers an enormous potential not only for neuromodulation, but is also a promising technique for many fields, such as cardiology and endocrinology. For example, expression of ChR2 in pancreatic β-cells resulted in a light-dependent secretion of insulin. This may be promising for a better understanding of diabetes mellitus [145]. Depolarisation of mouse cardiomyocytes was achieved by expressing and illuminating ChR2. This approach may help to study pace making or resynchronisation in cases of arrhythmia and it may provide a new opportunity for treatment [146, 147].

1.3.2 Constructs

1.3.2.1 Rhodopsins

Rhodopsins are proteins that contain a hydrophobic seven transmembrane domain. They exist in almost every species on earth. Every rhodopsin which has been investigated in recent years, consists of an opsin and a covalently bound chromophore e.g. retinal [137, 148]. Retinal is related to vitamin A and connects with the binding pocket of a rhodopsin. The binding pocket is framed by the seven transmembrane domain [149]. Retinal isomerises after the absorption of a photon. This conformational change of the molecule triggers ion transport, channel opening and other actions [150].

The opsin family can be divided into microbial rhodopsins (type I) and animal rhodopsins (type II). Type I rhodopsins are present in prokaryotes, algae and fungi. Ion pumps make up the majority of this group. They can store energy produced from light or act as photoreceptors that enable phototaxis [137]. Retinal

serves as the chromophore. Type II rhodopsins can be found in higher eukaryotes. They belong to the family of GPCRs. By means of signal cascades and transmitter molecules, they can manipulate the opening state of ion channels [149]. The genetic information for opsins is encoded in a single gene. Additionally, opsins do not have a significant dark activity [150] (4.4).

1.3.2.2 Channelrhodopsin

Chlamydomonas rheinhardtii is a green alga, that has a mean diameter of 8 µm and two flagella. The organism contains an orange tinted eye region. Already in 1916 it was known that the “eye” of the alga perceives light which affects the swimming behaviour of the organism [151]. The exact mechanism behind this phototactic behaviour of *Chlamydomonas* remained unclear. In the meantime, the cause has been revealed. Two rhodopsins were detected in the eye region of the alga [132]. They belong to a new kind of rhodopsins, called ChRs. The combination of an opsin with a chromophore, e.g. retinal, is termed a ChR (Chop1 + retinal = ChR1) [152]. ChRs are ion channels with an intrinsic light sensor and an own photocycle. They show similarities to existing rhodopsins, but so far there has not been an ion channel that can be activated by light. ChRs are the first channels containing a seven transmembrane domain [152]. The kinetics depend on the conductance state, light intensity, wavelength, the extinction coefficient as well as the quantum efficacy (the amount of photons that is necessary to achieve conformational change). It is convenient for experimental use that the cofactor retinal is present in every vertebrate tissue that has been tested so far [149].

The ChRs of *Chlamydomonas rheinhardtii*, termed ChR1 and ChR2, differ from each other (Table 2). Only monovalent ions can pass through the central pore of ChR1, in this case almost exclusively H^+ [135]. In contrast, ChR2 is permeable for mono- and divalent ions [153]. The photocurrent of ChR2 reaches its maximum at 470 nm excitation (blue light). Due to the cation transport, a depolarisation of the cell membrane can be achieved [139].

Table 2: Comparison of channelrhodopsins from *C. rheinhardtii*

	Channelrhodopsin 1	**Channelrhodopsin 2**
Ion conductance	H^+	H^+, Na^+, K^+, Ca^{2+}
Amino acids	712 (Chop1)	737/315 (Chop2)
Absorption maximum	510 nm	470 nm

Hegemann, P. (2005); Nagel, G. (2003); Sineshchekov, O. A. (2002); *personal communication*

In this project, a modified version of ChR2, called ChR2 D156C or ChR2-XXL, was used. It differs from ChR2 in the amino acid position 156, where cysteine was inserted instead of aspartic acid. ChR2-XXL is characterised by an extended open state, an improved subcellular localisation as well as an enhanced expression. Due to the extended open state, the light sensitivity is increased. This mutant can generate stronger photocurrents than the wild type. ChR2-XXL has an absorption maximum for photons (λ_{max}) at 477nm [154, 155]. The construct was kindly provided by the working group of Prof. Georg Nagel (Institute of Physiology, Chair II (Neurophysiology), JMU, Würzburg, Germany).

Nowadays, ChR2 is the most frequently used construct in optogenetics, especially in the neurologic field.

1.3.2.3 Anion channelrhodopsin

For a long time, ChRs from chlorophyte algae were the only channels used in the field of optogenetics. For the hyperpolarisation of cell membranes, light-driven ion pumps were used, such as archaerhodopsin-31 (Arch), an outward proton pump from *Halorubrum sodomense* or the inward chloride pump halorhodopsin (Halo/NpHR) from *Natronomas pharaonic* [130, 156]. Their disadvantage is that only one ion can be transported per photocycle and therefore continuous high light intensities are required. There have been attempts to generate more effective tools for the hyperpolarisation of cells. For this reason, ChRs were modified to transport anions, e.g. chloride. Nevertheless, no exclusive anion selectivity was achieved, because a small current of cations was still

present [157, 158]. In 2015, anion channelrhodopsins (ACRs), a new group of ChRs were discovered in marine algae. ACRs selectively transport anions and therefore can generate hyperpolarisation of the cell membrane [159]. Compared to anion or proton pumps, several ions can be transported per photocycle [160].

The construct, which was used in this project originated from the cryptophyte *Guillardia theta* and was kindly provided by the working group of Prof. Georg Nagel (Institute of Physiology, Chair II (Neurophysiology), JMU, Würzburg, Germany). Two subtypes can be distinguished from this species, *Guillardia theta* anion channel rhodopsin 1 (*Gt*ACR1) and *Guillardia theta* anion channel rhodopsin 2 (*Gt*ACR2). *Gt*ACR1 and *Gt*ACR2 respond to diverse ranges of spectra (*Gt*ACR1 515 nm; *Gt*ACR2 470 nm). 53 sequences were detected in *Guillardia theta*, which are similar to microbial rhodopsins (type I) [159]. The advantage of ACRs is that they already respond to lower light intensities. This is why, illumination time can be reduced, and tissue is not negatively affected by heat development [161]. Due to their high sensitivity, the expression rate of ACRs can also be lower, compared to other constructs [162].

Until now, 20 different ACRs from various marine organisms have been found. They differ in amplitude, kinetics and range of spectra of their photocurrents [163]. Some constructs have been utilised to suppress action potentials in neurons or to inhibit electrical activity in cardiomyocytes [163, 164].

1.3.2.4 Bacterial photoactivated adenylyl cyclase

It was known that *Euglenia gracilis* modified its swimming movements regarding changes in light and light intensity, but the mechanism remained unclear. A few years ago, a photoactivated adenylyl cyclase (PAC) was discovered in the unicellular flagellate *Euglenia gracilis*. It was named EuPAC and belongs to the group of flavin-binding photoreceptors [165] (Table 3). Flavin-binding receptors are sensitive to blue light (440-480 nm). On one hand, light with these wavelengths can harm organisms due to arising oxygen radicals [166]. On the other hand, it is a natural engine of photosynthesis and supports enzymes in the repair of damaged DNA [167]. PACs can produce the second messenger cAMP with the use of light [168]. The enzyme consists of two subunits, called PAC*alpha*

and PAC*beta* [165]. Both subunits contain two blue light using flavin adenine diphosphate (BLUF) domains each (Table 3) and are linked to an adenylyl cyclase [169]. Recently, another PAC was discovered in *Beggiatoa sp.* and was named bPAC. In contrast to EuPAC, bPAC only contains one BLUF domain that is connected to one adenylyl cyclase. An activation, even at low light levels, is possible, due to a slower photocycle. The DNA of bPAC is shorter than the DNA of the subunits EuPAC*alpha* and EuPAC*beta*, which facilitates the introduction into other organisms [170, 171]. With this instrument it is possible to manipulate the cAMP concentration in cells by light.

Table 3: Groups of flavin-binding photoreceptors

	occurance	**sensitivity**	**speciality**
Cryptochromes	various plants	blue light	receptor
BLUF (blue light using FAD) domains	proteobacteria, cyanobacteria	blue light	domain; uses flavin adenine dinucleotide (FAD)
LOV (light, oxygen, voltage) domains	plants, bacteria, microalgae, fungi	blue light	sensor protein; contains flavin chromophore

Christie, J. M. (1999); Gomelsky, M. & Klug, G. (2002); Lin, C. (1995); Raffelberg, S. (2013)

bPAC was tested in *E. coli*, in rat hippocampal pyramidal cells, in the central nervous system (CNS) of *Drosophila* and in oocytes of *Xenopus leavis*. Under blue light, it was possible to increase the enzyme activity up to 300-fold. Pure bPAC protein produced 10±2 nmol of cAMP/min/mg of protein during one minute of illumination with blue light. The maximum light sensitivity was detected at 441 nm [171].

The construct bPAC was kindly provided by the working group of Prof. Georg Nagel (Institute of Physiology, Chair II (Neurophysiology), JMU, Würzburg, Germany). The construct was fused to Glycophorin A and targeted to the membrane. Its dark activity was 10 times lower than the dark activity of wildtype

bPAC-eYFP. The light activity was also six times lower compared to bPAC-eYFP *(personal communication with Dr. Shiqiang Gao)*.

1.3.2.5 Photoactivated guanylyl cyclase

A light-activated guanylyl cyclase was found in the fungus *Blastocladiella emersonii*, whose zoospores showed phototactic behaviour. Originally, the cyclase is named BeGC1 [172]. In this thesis it will be called *Be*Cyclop, based on the suggestion of the working group of Prof. Georg Nagel (Institute of Physiology, Chair II (Neurophysiology), JMU, Würzburg, Germany), which kindly provided this construct.

*Be*Cyclop consists of a microbial (type I) opsin domain close to the N-terminal end and a guanylyl cyclase domain close to the C-terminal end. A yellow fluorescent protein (YFP) is fused to the C-terminal end. According to Gao *et al.* it is the first rhodopsin with eight transmembrane domains. Another difference to previously known rhodopsins is the intracellular N-terminal end. The optogenetic construct is sensitive to green, red and violet light, with a maximum sensitivity at 530 nm. By generating the second messenger cGMP, the guanylyl cyclase can increase the intracellular cGMP concentration. In membrane extracts of *Xenopus laevis* oocytes expressing *Be*Cyclop, a turnover of approximately 17 $cGMPs^{-1}$ was detected. The cGMP concentration in *Xenopus* oocytes increased up to 180- fold compared to oocytes that did not express the light-sensitive guanylyl cyclase. Furthermore, the function of the construct was tested in HEK 293T cells and body wall muscle cells of *C. elegans* [107].

1.4 Aim of the thesis

MK biology is only poorly understood. Until now, we do not know which factors trigger proplatelet formation or induce MK maturation. Nevertheless, the understanding of this process is fundamental for the development of new methods for platelet production *in vitro*. With the opportunity to generate platelets, the medical sector will be independent from blood donors. Additionally, platelet transfusions can be individually adapted to each patient to prevent antibody formation.

The aim of this study was to establish optogenetics in MKs. Furthermore, the focus laid on modulation of second messenger (cAMP/cGMP) concentrations and manipulation of ion conductance in MKs with light, because these factors seem to play an important role in MK differentiation and maturation.

Additionally, the results may help to shed new light on the mechanisms underlying thrombopoiesis, optimisation of MK cultivation and the improvement of platelet generation *in vitro*.

2 Material and methods

2.1 Material

2.1.1 Materials

Material	Manufacturer
18 G x 1 ½”, 20 G x 1 ½” needles	B. Braun (Melsungen, Germany)
26 G x 1 ½” needles	BD Biosciences (Heidelberg, Germany)
Canonical tube 15 ml	Greiner Bio-one (Kremsmünster, Austria)
Canonical tube 50 ml	Greiner Bio-one (Kremsmünster, Austria)
Cell cultivation plates 10 cm/ 6 cm	Greiner Bio-one (Kremsmünster, Austria)
Cell cultivation plates 6-well	Greiner Bio-one (Kremsmünster, Austria)
Cellulose acetate sterile filter 0.45 µm	Roth (Karlsruhe, Germany)
Easy strain sterile cell filter 100 µm	Greiner Bio-one (Kremsmünster, Austria)
Eppendorf tubes	Sarstedt (Nümbrecht, Germany)
Nunc™ Glass Base Dish	Thermo Fisher (Waltham, USA)
Nunclon™ Delta Surface	Thermo Fisher (Waltham, USA)
Precalibrated Pipettes	Hartenstein (Würzburg, Germany)

2.1.2 Chemicals

Chemical	Manufacturer
Anti-GFP (GFP (D5.1) XP Rabbit mAB) #2956	Santa Cruz sc-8334 (Dallas, USA)
Ampicillin	Roth (Karlsruhe, Germany)
Bovine Serum Albumin – Low Endotoxin (BSA)	AppliChem (Darmstadt, Germany)
Cilostazol	Sigma-Aldrich (Schnelldorf, Germany)
DH5α competent cells	Thermo Fisher (Waltham, USA) 18263012
Dimethylsulfoxide (DMSO)	Sigma-Aldrich (Schnelldorf, Germany)
Dipyridamole	Sigma-Aldrich (Schnelldorf, Germany)
Dulbecco's Phosphate Buffered Saline	Sigma-Aldrich (Schnelldorf, Germany)
Ethanol 70% denatured	Roth (Karlsruhe, Germany)
Fetal Calf Serum (FCS)	Thermo Fisher (Waltham, USA)
HCl	Roth (Karlsruhe, Germany)
Hexadimethrine	Sigma-Aldrich (Schnelldorf, Germany)
Isofluran CP®	Cp-pharma (Burgdorf, Germany)
Isopropanol	Roth (Karlsruhe, Germany)
LB plates containing Ampicillin (50 µg/ml)	own production
Mineral oil	Thermo Fisher (Waltham, USA)
Paraformaldehyde	Sigma-Aldrich (Schnelldorf, Germany)
Penicillin/Streptomycin (P/S)	Thermo Fisher (Waltham, USA)
Polyethylenimine (PEI)	Sigma-Aldrich (Schnelldorf, Germany)
Stem Cell Factor (SCF)	BioLegend (San Diego, USA)
StemPro®-34 Nutrient Supplement	Gibco (Karlsruhe, Germany)
StemPro®-34 Serum Free Medium	Gibco (Karlsruhe, Germany)
Streptomycin	PAN Biotech (Aidenbach, Germany)
Thrombopoietin (TPO) from cell supernatant	Nieswandt laboratory (Würzburg, Germany)
Triton X-100	AppliChem (Darmstadt, Germany)

2.1.3 Devices

Device	Manufacturer
Centrifuge 5415 R	Eppendorf (Hamburg, Germany)
Centrifuge 5424	Eppendorf (Hamburg, Germany)
Centrifuge 5810 R	Eppendorf (Hamburg, Germany)
Centrifuge Avanti J-25	Beckman Coulter (Brea, USA)
Centrifuge VWR Megastar 1,6 R	VWR International (Radnor, USA)
Kuhner Shaker X ISF-1-W	Kühner (Birsfelden, Switzerland)
Nanodrop one	Thermo Fisher (Waltham, USA)
Neubauer chamber	Marienfeld (Lauda-Königshofen, Germany)
Scale EL 303	Mettler Toledo (Columbus, USA)
TCS SP8 CLSM	Leica Microsystems (Wetzlar, Germany)
Zeiss Axiovert 40 CFL	Zeiss (Oberkochen, Germany)
Zeiss Observer Z1	Zeiss (Oberkochen, Germany)

2.1.4 Kits

Kit	Manufacturer
DetectX High Sensitivity Direct Cyclic AMP/GMP Chemiluminescent Immunoassay Kit	Arbor Assays (Ann Arbor, USA)
Plasmid Maxi Kit (25)	Qiagen (Hilden, Germany)

2.1.5 Mouse line

For BM-MK cell culture C57BL/6 mice were used. To obtain foetal liver cells (FLC), day 14 pregnant female CD1 mice from Charles River were used.

2.1.6 Media and buffers

- **LB medium, pH 7.5-8**

Tryptone	10	g/l
Yeast extract	5	g/l
NaCl	10	g/l

- **SOC medium**

Tryptone	2	%
Yeast extract	0.5	%
NaCl	10	mM
KCl	2.5	mM
$MgCl_2$	10	mM
$MgSO_4$	10	mM
Glucose	20	mM

- **CO_2 independent medium**

$CaCl_2$	110.00	mg/l
$CuSO_4$	0.0018	mg/l
$FeSO_4$	0.56	mg/l
$MgCl_2$	131.00	mg/l
$MgSO_4$	150.00	mg/l
KCl	330.00	mg/l
$NaHCO_3$	200.00	mg/l
NaCl	6000.00	mg/l
Na_2SeO_3	0.0067	mg/l
ZnSO4	0.44	mg/l

- **Methylcellulose-based CO_2 independent medium**

Methylcellulose	45	ml
CO_2-independent medium	135	ml
Added foetal calf serum	1	ml
Added L-Glutamine	10	µl

- **Phosphate-buffered saline (PBS), pH 7.14**

KCl	2.7	mM
KH_2PO_4	1.5	mM
NaCl	137	mM
Na_2HPO_4	8	mM

- **Extraction buffer (membrane activity), pH 7.3**

NaCl	100	mM
Tris-Cl	75	mM
Dithiothreitol (DTT)	5	mM
Glycerol	5	%

- **Reaction buffer (membrane activity), pH 7.3**

Guanosine triphosphate (GTP)	1	mM
$MgCl_2$	5	mM
NaCl	100	mM
Tris-Cl	75	mM
Dithiotreitol (DTT)	5	mM

Media and buffer	**Manufacturer**
S.O.C. medium	Invitrogen TM Thermo scientific fisher 15544034
DMEM high glucose GlutaMax™ supplement (cell culture medium)	Gibco TM Thermo Scientific Fisher 10566016
StemPro™ -34 SFM + supplement (BM-MK culture medium)	Gibco TM Thermo Scientific Fisher 10639011
CO_2 independent medium	Gibco TM Thermo scientific fisher 18045054

2.1.7 Lamps and boxes

Device	Manufacturer
RGB LED light chain, 12 V	Light & More (Forchtenberg, Germany)
MENGS E14 3W RGB LED	Shenzhen Procent Technology Co., Ltd. (Shenzhen, China)
Transport Box DuraPorter (red)	Roth (Karlsruhe, Germany)

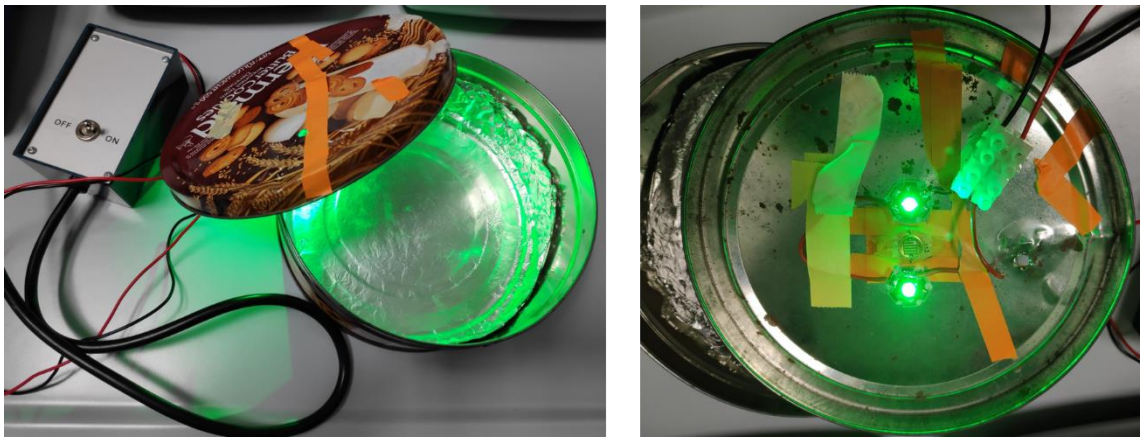

Figure 4: Custom-made box for cell illumination

2.2 Methods

2.2.1 Molecular biology

2.2.1.1 Retransformation with DH5*alpha* competent cells

Reaction tubes containing competent cells were thawed on ice. 1-10 ng DNA in 1-2 µl liquid were added to the cells. The tubes were then tapped and mixed gently. Following this, the cells were incubated on ice for 30 min. After incubation, the cells were heat shocked for 45 sec at 42°C and immediately placed on ice for 2 min. Subsequently, 450 µl of S.O.C. medium were added. The tubes were shaken at 225 rpm for 1 hour at 37°C. 100 µl of the cell dilution were spread on LB plates containing ampicillin (50 µg/ml), which were then incubated at 37°C overnight.

Next day, an autoclaved Erlenmeyer flask containing 150 ml of LB medium supplemented with 0,5 µl/ml ampicillin, was prepared for each construct. One colony of each construct was picked from the plate and added to the flask (one colony per flask). Erlenmeyer flasks were then shaken in an incubator at 220 rpm and 37°C overnight.

2.2.1.2 Plasmid purification

A Plasmid Maxi Kit (Qiagen) was used for purification. The bacterial culture was centrifuged at 6.000xg for 15 min at 4°C. After this, the bacterial pellet was resuspended in 10 ml Buffer P1. Additionally, 10 ml Buffer P2 were added. The solution was mixed by inverting the tube 4-6 times. Afterwards, the tubes were incubated for 5 min at room temperature. 10 ml prechilled Buffer P3 were then added. Again, the solution was mixed by inverting the tube vigorously. The tube was incubated on ice for 20 min. The liquid was then centrifuged at 20.000xg for 30 min at 4°C. Following this, a Qiagen-tip 500 was equilibrated using 10 ml Buffer QBT. The supernatant was applied and entered the column by gravity flow. Next, the Qiagen-tip was washed with 2x30 ml QC Buffer. The DNA was eluted with 15 ml QF Buffer into a clean 50 ml tube. Subsequently, the DNA was precipitated by adding 10.5 ml isopropanol at room temperature. The solution

was centrifuged at 15.000xg for 30 min at 4°C. The supernatant was then decanted carefully. After that, the DNA pellet was washed with 5 ml 70% ethanol at room temperature. Once more, the liquid was centrifuged at 15.000xg for 10 min and the supernatant was carefully decanted. Finally, the pellet was air-dried for about 10 min and dissolved in highly purified water.

2.2.2 Transfection (virus production)

About $5x10^6$ HEK 293T cells were seeded into a 10 cm Nunclon™ Delta Surface plate 24 hours before transfection. The next day, the culture medium was removed, and 4 ml of fresh cell culture medium were carefully added to the plate. The transfection mix was prepared, containing 10 µg of the vector (optogenetic construct), 10 µg pCL plasmid and 60 µl polyethyleneimine (PEI). The solution was filled up to 1 ml with cell culture medium without additives. Subsequently, the transfection mix was vortexed and incubated for 20 min at room temperature. Afterwards, the transfection mix was added dropwise (1 ml onto a 10 cm plate) and the plate was carefully moved to mix the transfection reagent into the medium. From then on, all steps were performed under red light in order to prevent activation of the light-sensitive proteins. After 5 hours of incubation, the transfection medium was replaced with 5 ml of fresh cell culture medium. 48 hours after transfection the supernatant was collected, if the transfection rate was sufficient. An Axiovert 40 CFL Zeiss microscope was used to validate the fluorescence of the HEK 293T cells. Subsequently, the supernatant was filtered with a 0.45 µm syringe filter and was stored in 1 ml aliquots at -80°C.

2.2.3 Cultivation of BM-derived MKs

The mice were anaesthetised with isoflurane by inhalation. They were sacrificed by cervical dislocation. After this, both femora were prepared and put into a plate filled with phosphate buffered saline (PBS). The epiphyses of the bones were cut in order to flush out the BM using a 26 G needle. It was collected in a dish containing 5 ml of culture medium. To prepare a single cell suspension, the solution was carefully homogenised using needles with decreasing diameters (18-26 G). To remove solid tissue parts the solution was passed through a falcon

cell strainer (100 µm) into a 50 ml canonical tube. The strainer was washed with 2 ml of medium. Following this, the cell solution was centrifuged at 200xg for 5 min at room temperature. Afterwards, the medium was removed, and the cells were resuspended in 5 ml fresh culture medium, supplemented with 50 ng/ml of stem cell factor (SCF). The cells were cultured for two days in a 60 mm x 15 mm petri dish at 37°C and 5% CO_2.

On day two, the cells were transferred into a 15 ml canonical tube and the dish was washed with 5 ml culture medium. Subsequently, the cells were centrifuged at 220xg for 5 min at room temperature. The cells were resuspended in 5 ml fresh culture medium supplemented with 50 ng/ml SCF and 5 µl/ml thrombopoietin (TPO). Again, the cells were cultured for 2 days.

2.2.3.1 Transduction

On day four, the suspension was divided up into different tubes, depending on how many experimental conditions were chosen. The cells were centrifuged at 200xg for 5 min at room temperature. Afterwards, the cells were resuspended in 1.5 ml culture medium supplemented with 10 µg/ml hexadimethrine (Polybrene®). 1 ml retroviral supernatant was added. The samples were transferred into a 6-well plate and centrifuged at 800xg for 90 min at room temperature. The following steps were performed under red light. After centrifugation, the wells were incubated for 90 min at 37°C and 5% CO_2. The cell suspensions were collected into 15 ml canonical tubes and centrifuged once more at 200xg for 5 min at room temperature. The cells were resuspended in 2 ml fresh culture medium supplemented with 50 ng/ml TPO and cultured in a new 6- well plate for 1 day at 37°C and 5% CO_2.

2.2.3.2 Bovine serum albumin density gradient

On day 5, the cell suspensions were collected and centrifuged at 200xg for 5 min at room temperature. Excess culture medium was removed except for the last millilitre. A 1.5-3.0% bovine serum albumin (BSA) fraction single step gradient was prepared for each sample in order to isolate MKs. For this, 1.5 ml 3% BSA, dissolved in PBS, followed by 1.5 ml 1.5% BSA in PBS, were added to a 15 ml

canonical tube. The cell suspensions were resuspended and carefully layered on top of the gradient. After 30 min at 37°C and 5% CO_2 the gradient was removed without disturbing the MK pellet. Finally, the cells were resuspended in 2 ml culture medium supplemented with 50 ng/ml TPO.

Table 4: BM-derived MK cultivation schedule

Day	Task
0	Isolation of BM; cell cultivation
2	Exchange of culture medium
4	Transduction with retrovirus; subsequent steps under red light
5	BSA-gradient for BM-derived MK enrichment
6	cAMP/cGMP determination
7	Incubation microscopy

Table modified from Bachelor Thesis of Nauroth, C. (2016). Optogenetic approaches to study platelet production.

2.2.4 Cultivation of FLC-derived MKs

Time mated CD1 female mice (day 14) were used to obtain FLCs. The mice were anaesthetised with isoflurane by inhalation and sacrificed by cervical dislocation. The abdomen was opened, and every single foetus was removed and put into a well filled with PBS. Hereafter, the foetal livers were carefully separated from tissue parts. One foetal liver was put into a well of a 6-well plate filled with 2 ml of cell culture medium (DMEM). To prepare a single cell suspension, the solution was carefully homogenised using needles with decreasing diameters (18-26 G). Afterwards, the solution was passed through a cell strainer (100 µm) into a 50 ml canonical tube to remove solid tissue parts. The well and strainer were rinsed with 5 ml of cell culture medium (DMEM). Subsequently, the solution was centrifuged at 200xg for 5 min at room temperature. Finally, the cells were

resuspended in 2 ml of fresh culture medium supplemented with 50 ng/ml TPO. The 6-well plates were incubated for two days at 37°C and 5% CO_2.

On day 2, transduction was performed according to the transduction protocol for BM-derived MKs (2.2.3.1), with the only difference that cell culture medium (DMEM) was used for the cultivation of FLCs.

On day 3, a BSA density gradient was used to isolate FLC-derived MKs. It was performed according to the protocol for BM-derived MKs (2.2.3.2).

Table 5: FLC-derived MK cultivation schedule

Day	Task
0	Isolation of FLCs; cell cultivation
2	Transduction with retrovirus; subsequent steps under red light
3	BSA-gradient for FLC-derived MK enrichment
4	cAMP/cGMP determination
5	Incubation microscopy

Table modified from Bachelor Thesis of Nauroth, C. (2016). Optogenetic approaches to study platelet production.

2.2.5 Optogenetic experiments with MKs

2.2.5.1 Confocal microscopy

All samples for confocal microscopy were prepared under red light. First, a solution of 4% paraformaldehyde (PFA) supplemented with 0.1% Triton-X 100 was prepared. MKs were carefully removed from the culture dish with a cut pipette tip in order to avoid damage of proplatelets. 200 µl of the cell solution were combined with 200 µl of the PFA mix. Until imaging, the samples were kept in the fridge. Images were taken with a TCS SP8 CLSM microscope from Leica.

2.2.5.2 Measurement of cAMP and cGMP concentration in MKs

All steps were carried out under red light. The cell count of each sample was determined using a Neubauer counting chamber or by performing a Bradford assay. For this, 20 µl of each sample were used. Afterwards, the samples for one condition were centrifuged at 200xg for 5 min at room temperature and the cell pellet was resuspended in 90 µl PBS. If used, an inhibitor was added at this timepoint. After 2 min of incubation, the samples were exposed to light in a custom-built box (Figure 4). To terminate the reaction, 30 µl of 0.4 M HCl were added. The samples were immediately frozen in liquid nitrogen and stored on dry ice.

Measurements of cAMP and cGMP concentration were performed by Dr. Shiqiang Gao and his colleagues (Institute of Physiology, Chair II (Neurophysiology), JMU, Würzburg, Germany). The samples were heated up to 95°C for 5 min. They were then vortexed and centrifuged at 10.000 rpm for 10 min. The supernatant was used to measure cAMP or cGMP concentration using a DetectX High Sensitivity Direct Cyclic AMP/GMP Chemiluminescent Immunoassay Kit.

2.2.5.3 Measurement of membrane activity

BM-derived MKs expressing *Be*Cyclop-eYFP were homogenised in extraction buffer using a pestle for microtubes. To remove bigger pellets as well as cell debris the solution was centrifuged at 200xg for 10 min. The membrane fraction was collected by centrifugation at 30.000xg for 10 min and resuspended in extraction buffer. The membrane suspension was added to the reaction buffer in a ratio of 1:10. The activity of *Be*Cyclop-eYFP was tested under dark and green light (532 nm, ~ 0.1 mW/mm^2). After different time points, the reaction was stopped with 0.1 M HCl. The concentration of cGMP was determined using a DetectX High Sensitivity Direct Cyclic GMP Chemiluminescent Immunoassay Kit. The measurements were performed by Dr. Shiqiang Gao and his colleagues (Institute of Physiology, Chair II (Neurophysiology), JMU, Würzburg, Germany).

2.2.5.4 Incubation microscopy

The coverslip of a Nunc™ Glass Bottom Dish coverslip was blocked with 3% BSA in PBS for 20 min at 4°C and was washed once with PBS. In the meantime, the cell suspension was spun down at 200xg for 5 min and then resuspended in 100 µl CO_2 independent medium. After transferring the cells into the Nunc™ Glass Bottom Dish, they were incubated for 15 min at 37°C and 5% CO_2. The cells were carefully covered with 200 µl methylcellulose-based CO_2 independent medium. Finally, the culture dish was overlaid with 1 ml of mineral oil. Before starting the observation, the dish was left to rest for about 10 min in order to let the cells settle down. A Zeiss Observer Z1 was used for imaging.

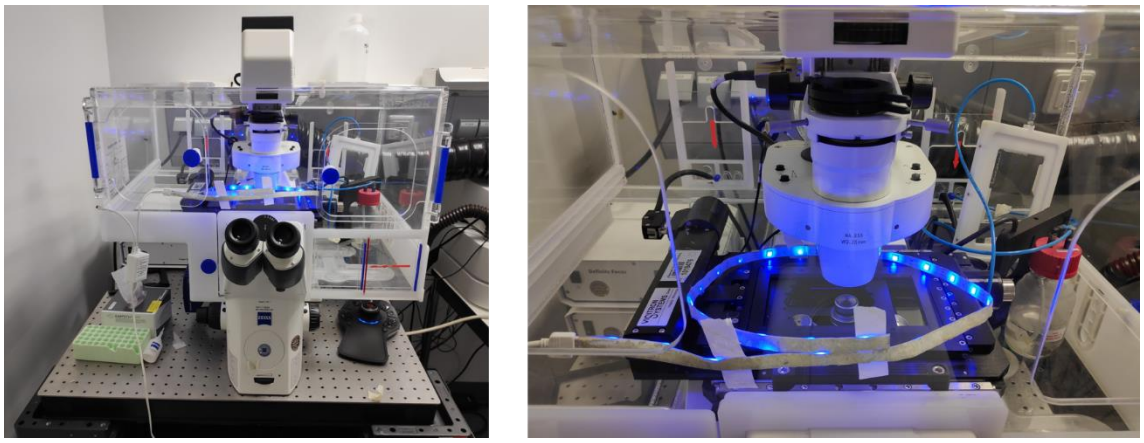

Figure 5: Set-up for incubation microscopy: microscope with LED light chain

2.2.6 Analysis

2.2.6.1 Programmes

Software	Manufacturer
GraphPad Prism	GraphPad Software
Image J	Open source Developer: Wayne Rasband (National Institutes of Health, Maryland, USA)

2.2.6.2 Statistics

Results are shown as mean values ± standard deviation (SD) from one experiment. Significant differences were determined using students-t-test. P-values <0.05 were considered as statistically significant: $p<0.05$ (*), $p<0.01$ (**), $p<0.001$ (***) and $p<0.0001$ (****). Results with a p-value >0.05 were considered not significant.

3 Results

Table 6: Construct designations

Official name	Abbreviation
ChR2 D156C-eYFP	ChR2-XXL
*Gt*ACR1-eYFP	*Gt*ACR1
*Be*Cyclop-eYFP	*Be*Cyclop
Glyco-eYFP-bPAC S27A	bPAC

For a better understanding, the following text uses the designations from the right column of the table.

3.1 Expression of optogenetic tools in MKs

First, it had to be proven that the light-sensitive proteins can be expressed in MKs. Therefore, the constructs (Table 6) were detected with an anti-YFP antibody. DAPI was used to stain the nucleus. Non-transduced cells only display a blue stained nucleus in the images. The intensity of the construct expression varied between cells. In order to better understand the effects of light-sensitive proteins, it is essential to know where they are expressed in the cells.

3.1.1 Light-sensitive ion channels

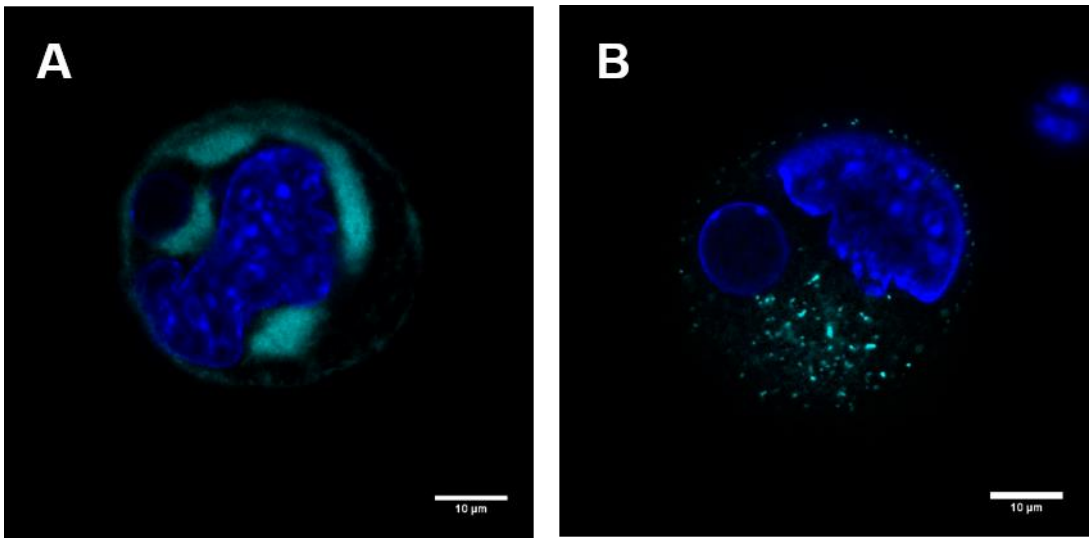

Figure 6: Localisation of ChR2-XXL and *Gt*ACR1 in BM-derived MKs

Representative images of BM-derived MKs expressing A: ChR2-XXL (cyan) or B: *Gt*ACR1 (cyan), DAPI (blue)

ChR2-XXL, an ion channel, is expected to be expressed in MK membranes. This not only includes the plasma membrane but also the invaginated DMS, a membrane reservoir for future platelets. Through tubular membrane connections it is in contact with the MK plasma membrane. Confocal microscopy images show that ChR2-XXL is present in the plasma membrane of MKs (Figure 6 A). The protein is also expressed in some areas close to the lobulated nucleus, suggesting localisation of ChR2-XXL in the DMS.

*Gt*ACR1 is an ion channel and is expected to be expressed in MK membranes as well. The strongest expression was found in the centre of the MKs and appears in a dotted pattern (Figure 6 B). Only a sporadically expression was detected in the plasma membrane.

3.1.2 Photoactivated cyclases

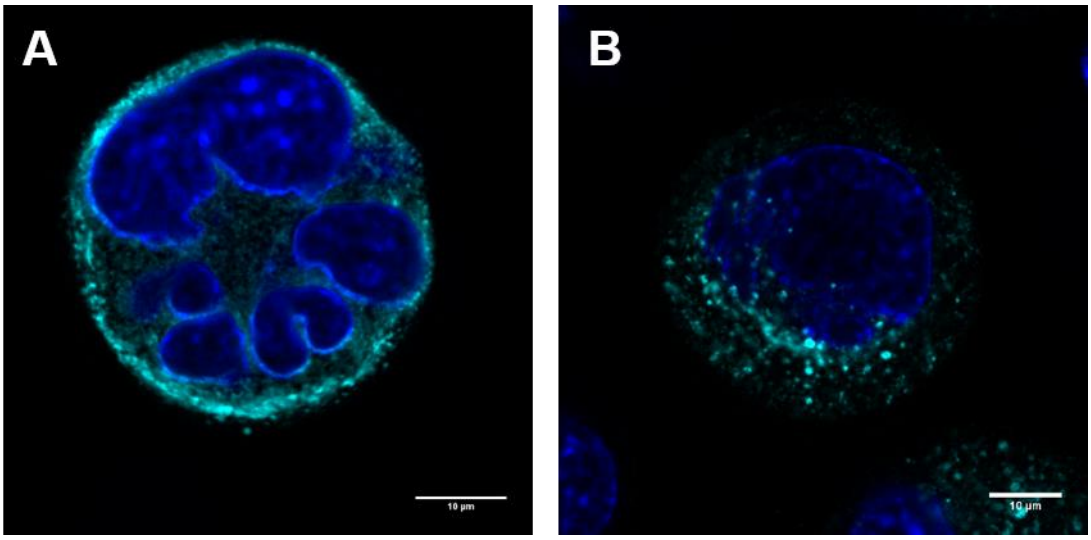

Figure 7: Localisation of *Be*Cyclop and bPAC in BM-derived MKs

Representative images of BM-derived MKs expressing A: *Be*Cyclop (cyan) or B: bPAC (cyan), DAPI (blue)

Fluorescence signal distribution of *Be*Cyclop was observed all over the cell. The strongest expression was detected close to the plasma membrane (Figure 7 A).

The expression of bPAC appeared in a dotted pattern (Figure 7 B). The protein was ubiquitously present in the cell except the nucleus. The expression seemed to be strongest, close to the nucleus. No continuous expression was detected in the plasma membrane.

3.2 Increase of cAMP and cGMP concentration in MKs after illumination

3.2.1 bPAC

3.2.1.1 cAMP concentration can be increased by light in FLC-derived MKs expressing bPAC

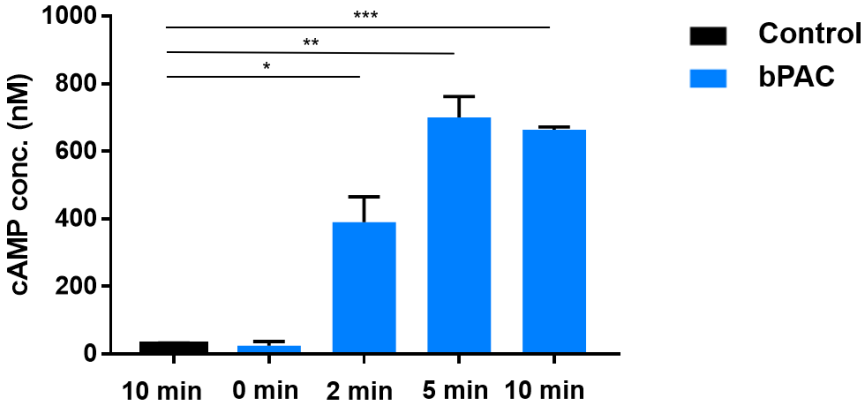

Figure 8: Determination of cAMP concentration in FLC-derived MKs expressing bPAC after illumination

Cells were illuminated with blue light for 0-10 min, *p<0.05, **p<0.01, ***p<0.001

It was shown that bPAC increases the cAMP level in different cell types after illumination [171, 173]. To determine whether light can increase the cAMP concentration in MKs, different illumination times were chosen. Non-transduced cells served as controls. Four different time intervals for illumination with blue light ranging from 0 to 10 min were tested. After the indicated time intervals, the reaction was stopped immediately, and the cAMP concentration was determined. The maximum value of 700.43±50.3 nM cAMP concentration was reached after 5 min of illumination (Figure 8). Thereafter, the detected levels decreased. For this reason, the illumination time of 5 min was used for the following experiments. In general, it was shown that cAMP levels can be increased in FLC-derived MKs expressing bPAC.

3.2.1.2 High activity of PDEs might be responsible for fast degradation of cAMP in MKs

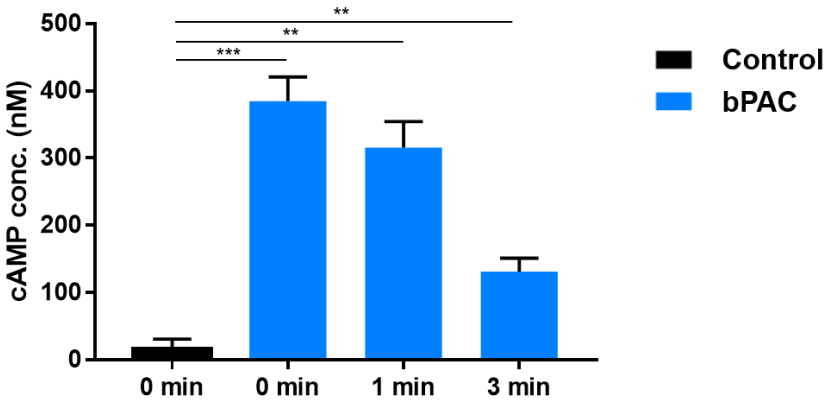

Figure 9: Determination of cAMP concentration in BM-derived MKs expressing bPAC

Cells were illuminated with blue light for 5 min and lysed at different timepoints (0-3 min), **p<0.01, ***p<0.001

To find out whether the duration between the end of illumination and the termination of the reaction had an influence on the cAMP concentration, different time points for cell lysis (0-3 min) were tested after illumination. The cells were illuminated with blue light for 5 min. No detectable increase of cAMP was measured in non-transduced cells, which served as control. In comparison there was a significant increase of the cAMP level in MKs expressing bPAC (Figure 9). The maximum of 384.67±29.49 nM cAMP concentration was reached at the lysis timepoint of 0 min (direct lysis after illumination). It was striking that the cAMP concentration decreased the longer the period between the end of illumination and the termination of the reaction lasted. The lowest cAMP concentration 131±16.39 nM was measured after the interval of 3 min. This data suggests that the duration between the end of illumination and the termination of the reaction is crucial. A potential explanation for this might be the activity of PDEs in MKs [116]. These enzymes are responsible for the degradation of the second messengers cAMP and cGMP in cells. To test whether PDEs in MKs are responsible for a faster decrease of cAMP levels after illumination, MKs were incubated with PDE inhibitors prior to illumination.

3.2.1.3 Treatment of FLC-derived MKs expressing bPAC with cilostazol slightly increases cAMP concentration after illumination

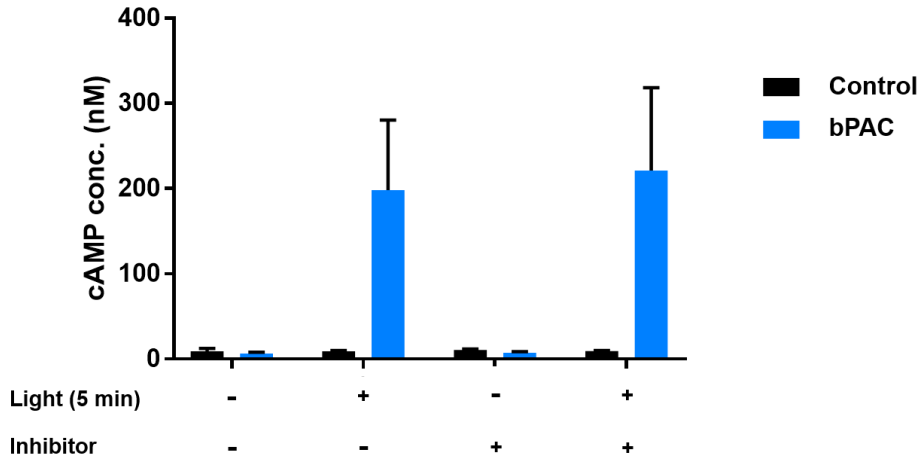

Figure 10: Determination of cAMP concentration in FLC-derived MKs expressing bPAC

Cells were illuminated for 5 min with blue light in the presence or absence of 1 µM cilostazol

Next, to test whether the combination of illumination and the use of a PDE inhibitor increases the cAMP concentration in MKs more effectively, cilostazol was used to inhibit PDE 3 activity. This enzyme has a major effect on degradation of intracellular cAMP [116]. Non-transduced cells served as controls for every condition. DMSO was used instead of cilostazol for control samples. Cilostazol or DMSO were added to the cells before illumination. After 2 min of incubation, each sample was illuminated with blue light for 5 min. The reaction was stopped immediately after the illumination time of 5 min. The control samples showed no increase of cAMP, whereas cAMP levels in transduced MKs increased up to 198±67.38 nM after illumination (Figure 10). In combination with PDE 3 inhibitor cilostazol, cAMP levels of 221±79.7 nM were determined. However, due to low sample numbers the data was not significant.

3.2.2 *Be*Cyclop

3.2.2.1 cGMP concentration can be increased by light in BM- and FLC-derived MKs expressing *Be*Cyclop

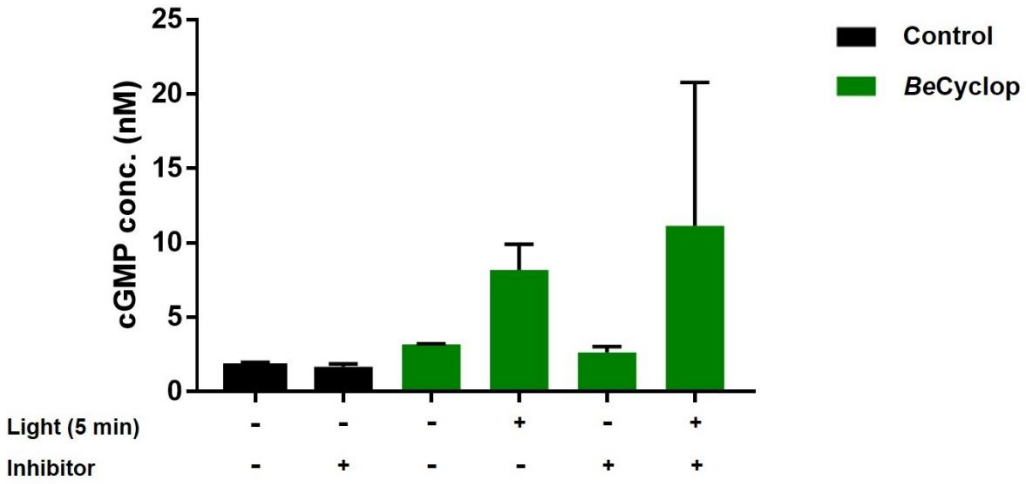

Figure 11: Determination of cGMP concentration in BM-derived MKs expressing *Be*Cyclop

Cells were illuminated with green light for 5 min in the presence or absence of 1 µM dipyridamole

Illumination of MKs expressing *Be*Cyclop for 5 min increased the cGMP concentration from 1.7±0.37 nM (0 min light) to 8.16±1.43 nM (5 min light) (Figure 11). To test the ability to further increase the intracellular cGMP levels in BM-derived MKs with light, dipyridamole was used as PDE inhibitor. This chemical is an inhibitor of PDE 5 and has a great impact on the degradation of cGMP [116]. Instead of dipyridamole, control samples were treated with the same volume of DMSO. Dipyridamole or DMSO were added to the cells 2 minutes before illumination. Each sample was illuminated with green light for 5 min. Subsequently, the reaction was stopped, and the cGMP concentration was determined. The combination of illumination and treatment with the inhibitor resulted in a cGMP concentration of 11.13±7.88 nM. However, the cGMP concentration varied greatly for this condition. In general, the overall values of cGMP (Figure 11) were much lower than those of cAMP in MKs expressing bPAC (Figure 9; Figure 10). Compared with the results obtained in FLC-derived MKs (Figure 12), no significant difference in the level of cGMP concentrations

could be detected. Nonetheless, it was possible to increase the cGMP concentration (Figure 11; Figure 12).

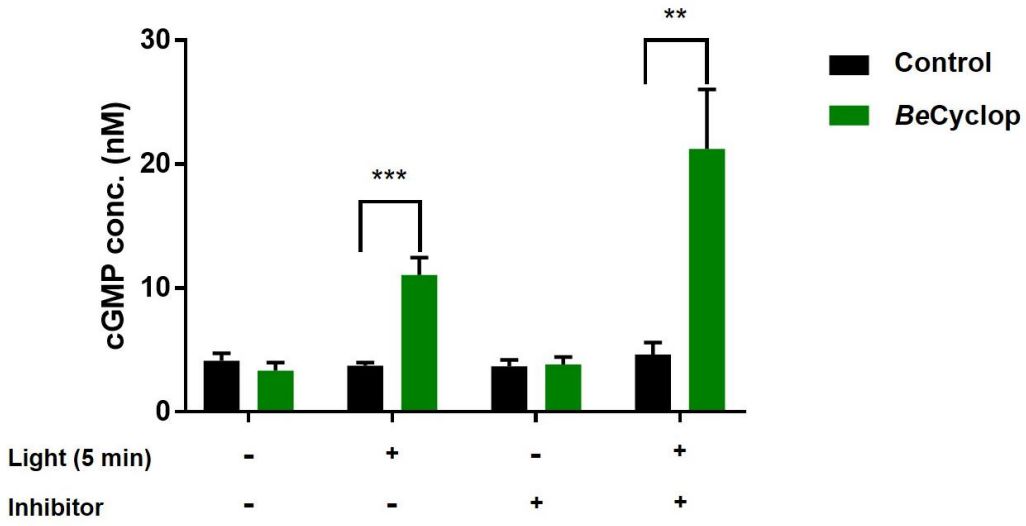

Figure 12: Determination of cGMP concentration in FLC-derived MKs expressing *Be*Cyclop

Cells were illuminated with green light for 5 min in the presence or absence of 1 µM dipyridamole, **p<0.01, ***p<0.001

Next, transduced and non-transduced FLC-derived cells were analysed using the following conditions: with or without illumination (5 min of green light) and in the presence or absence of dipyridamole or DMSO. The reaction was stopped immediately after 5 min of illumination. The results confirmed the assumption, that the cGMP levels in non-illuminated cells remained the same, whether or not the inhibitor was used. A significant increase up to 11.07±1.15 nM in cGMP was detected in illuminated cells. The combination of illumination and dipyridamole achieved values up to 21.23±4.21 nM cGMP (Figure 12). These results show that in both BM- and FLC-derived MKs expressing *Be*Cyclop the cGMP concentration can be increased after illumination. Treatment with the PDE 5 inhibitor dipyridamole further increases the concentrations of illuminated cells indicating that PDE 5 hydrolyses cGMP in MKs.

3.3 Determination of membrane activity of *Be*Cyclop in MKs

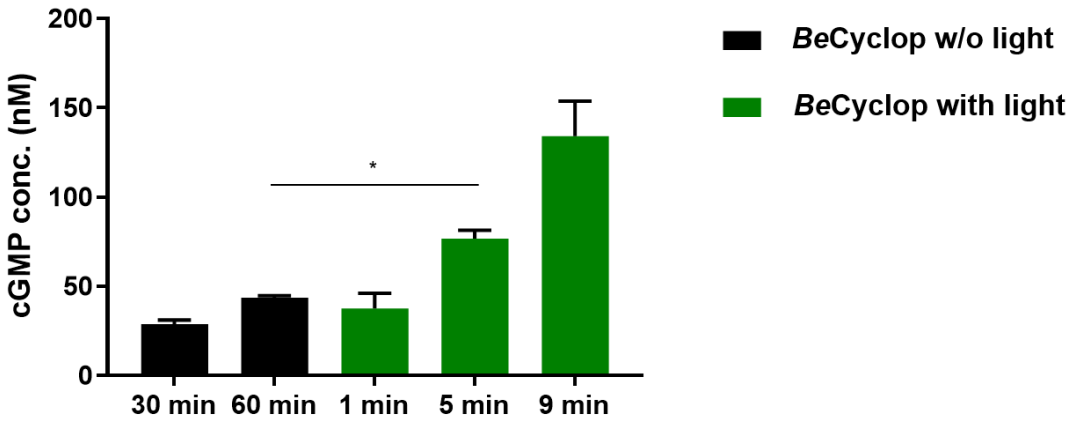

Figure 13: Determination of cGMP levels in BM-derived MKs expressing *Be*Cyclop

Membrane crude extract was exposed to different dark and light conditions, *p<0.05

It is assumed that PDEs are highly active in MKs. This is probably why the overall cGMP values were not as high as those of cAMP in the previous experiments. Therefore, an experiment was performed in which the influence of PDEs on the cGMP concentration was reduced [107]. Crude membrane extracts were prepared, to remove PDE proteins and their activity from the MK cytosol. The experiment was carried out in collaboration with the working group of Prof. Georg Nagel (Institute of Physiology, Chair II (Neurophysiology), JMU, Würzburg, Germany). Non-illuminated cells showed only a slight, non-significant increase from 28.8±1.6 nM cGMP (after 30 min) to 43.6±1.13 nM cGMP after 60 min. In contrast, 9 min illumination of the membrane extract strongly increased the cGMP concentration to 134±14 nM (Figure 13). These results reveal, that *Be*Cyclop can raise the cGMP concentration in BM-derived MKs even more, after reducing the influence of PDEs. The levels of the second messenger cGMP were raised more than 4-fold (28.8±1.6 nM cGMP to 134±14 nM cGMP) as compared to the initial value (30 min without light).

3.3.1 Conclusions I

In summary, the results show, that an expression of all four optogenetic constructs (ChR2-XXL, *Gt*ACR1, *Be*Cyclop and bPAC) was successfully achieved in MKs. Furthermore, it was possible to raise the cAMP and cGMP concentration with light in BM-derived MKs as well as in FLC-derived MKs that expressed the photoactivated cyclases bPAC and *Be*Cyclop. The low values of the second messengers may indicate a high activity of PDEs in MKs.

3.4 Proplatelets of MKs expressing light-sensitive ion channels retract during illumination

3.4.1 Proplatelets of FLC-derived MKs expressing ChR2-XXL retract during illumination

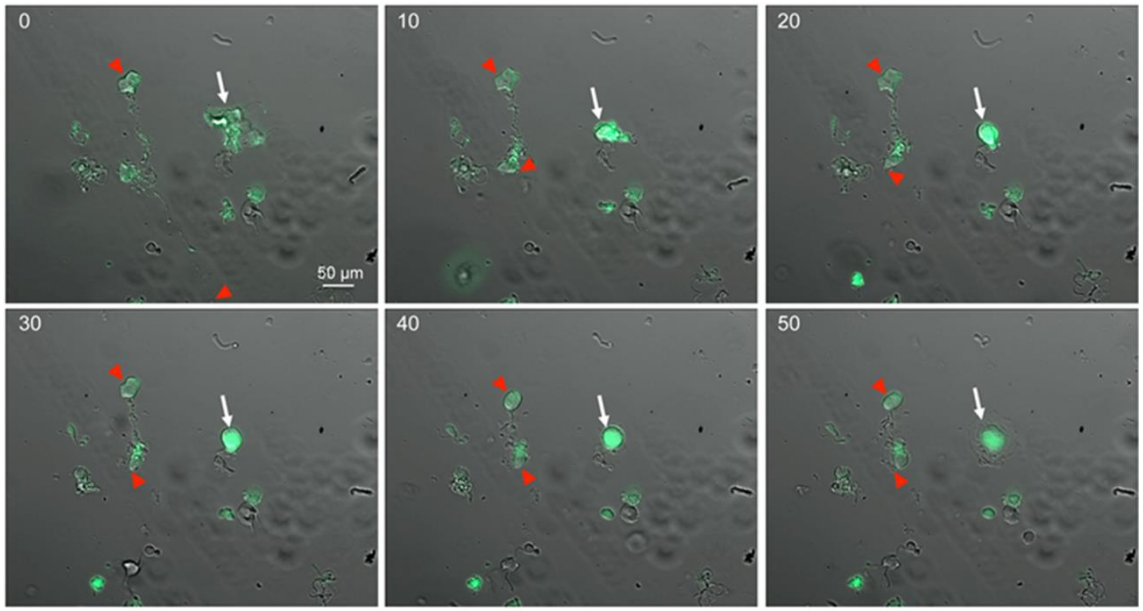

Figure 14: Representative images of a 50 min observation of illuminated FLC-derived MKs expressing ChR2-XXL

White arrow indicates spreading MK. Red arrow heads indicate the ends of a proplatelet. Numbers in upper left corner indicate time in minutes

ChR2-XXL is a cation channel and therefore triggers cation influx into the cell, when illuminated. To investigate whether the cation influx has an influence on MK behaviour, MKs were observed for 60 min during illumination (Figure 14). The concrete composition of the medium can be found in the material section (2.1.6). Proplatelets of FLC-derived MKs expressing ChR2-XXL retracted over time during illumination. The same MK is shown at different timepoints during 50 min of observation. FLC-derived MKs transduced with ChR2-XXL are depicted in green. Red arrow heads mark the ends of one proplatelet, which reduced in length over time. Furthermore, it was observed that MKs modified their shape and started to spread, which is highlighted by the white arrow.

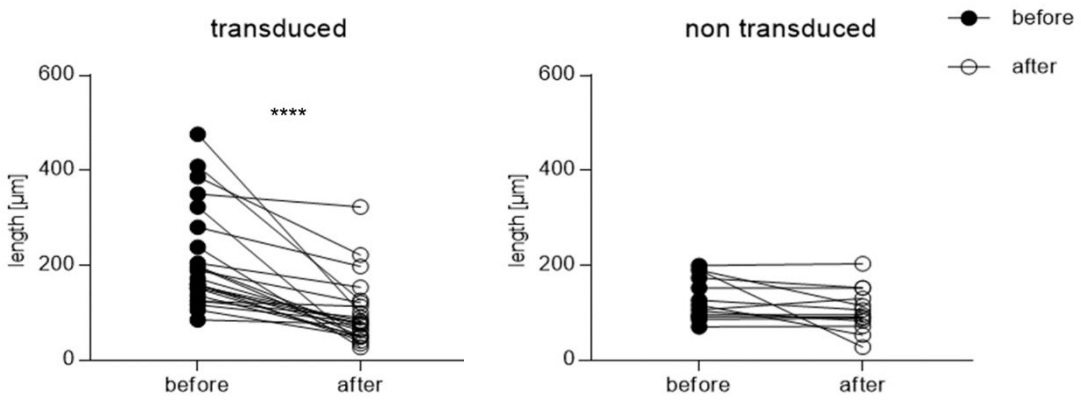

Figure 15: Determination of proplatelet length of control and ChR2-XXL expressing FLC-derived MKs before and after illumination

Measurements of proplatelet length were performed before and after 60 min of illumination, ****p<0.0001

Proplatelet length of FLC-derived MKs transduced with ChR2-XXL were analysed (Figure 15). Therefore, the proplatelet length of 38 transduced and 19 non-transduced cells was measured and compared. The measurements were taken at the beginning (0 min) and at the end (60 min) of the observation. A significant reduction in proplatelet length of transduced MKs over time was detected. 86.84% of the transduced cells reduced their proplatelet length by at least 10%, 60.25% by at least 50%. Only half of the non-transduced MKs (47.3%) reduced their proplatelet length by 10% and only 10.53% by 50%. This data suggests that cation influx has a negative impact on proplatelets and induces retraction of formed proplatelets into the cell body.

3.4.2 Proplatelets of FLC-derived MKs expressing *Gt*ACR1 retract during illumination

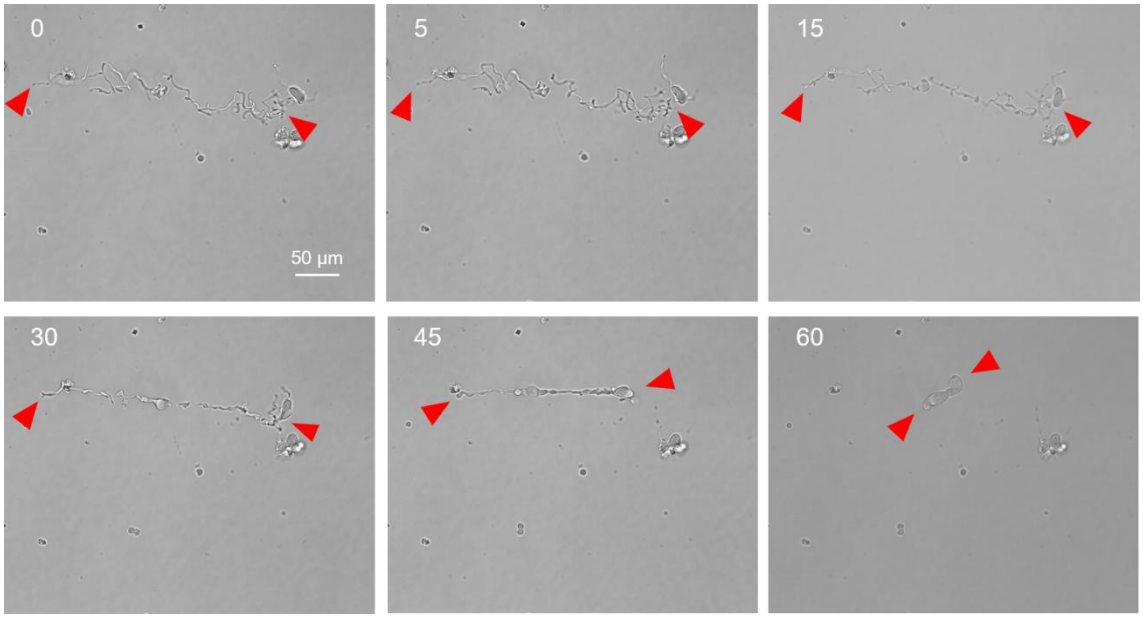

Figure 16: Representative images of a 60 min observation of illuminated FLC-derived MKs expressing *Gt*ACR1

Red arrow heads indicate the ends of a proplatelet

As an anion channel, ACR enables anion influx into cells, when activated by light. It was investigated whether a rise of the anion concentration in MKs has a similar effect on proplatelet behaviour as a rise of cation concentration (Figure 14). The expression of *Gt*ACR1 resembled a dotted pattern (Figure 6 B). Therefore, the transduction faded immediately or appeared rather weak in the images. Due to this fact, it was not possible to make the transduction visible in figure 16. Nevertheless, retracting proplatelets of *Gt*ACR1 expressing MKs were observed, highlighted by red arrow heads (Figure 16). It is striking, that after 15 min the small branched protrusions of the proplatelet retract into the main protrusion. After 30 min, there is only one almost straight proplatelet left. The main proplatelet starts retracting towards the cell body after 45 min.

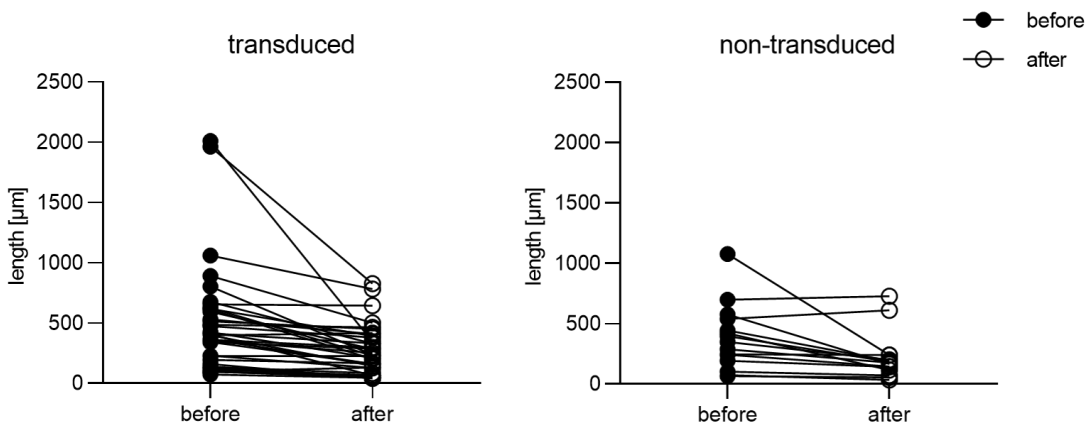

Figure 17: Determination of proplatelet length of control and *Gt*ACR1 expressing FLC-derived MKs before and after illumination

Measurements of proplatelet length were performed before and after 60 min of illumination

To test for the previously made observation with MKs expressing ChR2-XXL (Figure 15), proplatelet length of 39 transduced (*Gt*ACR1) and 15 non-transduced MKs was measured. The measurements were performed at the beginning (0 min) and at the end (60 min) of the illumination. Surprisingly, already 93.3% of the non-transduced cells reduced their proplatelet length by 10%, and 40% of the non-transduced cells reduced their proplatelet length by 50%. This is in marked contrast to what has been observed for the control cells in the experiments with ChR2-XXL. The retraction rate of proplatelets expressing *Gt*ACR1 was therefore comparable with 84.26% and 43.59% retracting about 10% and 50% respectively (Figure 17). However, since already the control cells showed a marked proplatelet retraction rate, it is difficult to conclude something about the effect of anion influx on proplatelet retraction.

3.4.3 Conclusions II

It was possible to express the ion channels ChR2-XXL and *Gt*ACR1 in FLC-derived MKs. A significant increase in retraction of proplatelets was detected for ChR2-XXL expressing MKs during an illumination period of 60 min. MKs expressing *Gt*ACR1 did not display any significant differences in retraction length, however surprisingly, the control cells already showed an unusual high rate of proplatelet retraction. Taken together, ChR2-XXL strongly influences MK behaviour via cation influx.

4 Discussion

So far, the cellular and molecular mechanisms of MK maturation and platelet production are only poorly understood. It has been shown that optogenetics is a valuable tool to manipulate cells in a non-invasive way by light [120]. It may also be a chance for the identification of key regulators in MK homeostasis and proplatelet formation. There are indications that the second messengers cAMP/cGMP and the effects of ions are important for MK maturation and proplatelet formation [78, 79, 112]. In this thesis, optogenetics was established in MK biology in order to manipulate second messenger and ion concentrations in these cells. Intracellular cAMP and cGMP concentrations increased strongly with the help of light-sensitive cyclases. Furthermore, the retraction of proplatelets of MKs expressing light-sensitive ion channels as well as MK spreading was observed.

These first data show, that it is possible to regulate cellular responses in MKs with the help of light. They form the basis for further experiments to better understand MK differentiation and to find possible triggers of proplatelet formation. However, there are many approaches to improve and optimise these results which are discussed below.

4.1 Impacts of increasing cAMP and cGMP concentrations on MKs and regulation of PDE activity

bPAC is a light-sensitive adenylyl cyclase with a BLUF domain. The cyclase is activated by blue light and produces the second messenger cAMP. The functionality of the light-sensitive enzyme has been tested in various fields of application. Previous investigations have shown that the injection of bPAC into *Xenopus* oocytes led to an increase of intracellular cAMP concentration after 1 min of illumination. Elevated cAMP in the *Drosophila* CNS stops their grooming behaviour. Expression of bPAC in the CNS of transgenic *Drosophila* made it possible to stop their grooming after a short light pulse [171]. This was an indication that the cyclase is functional *in vivo*. Furthermore, expression of bPAC in pituitary cells of transgenic zebrafish activated the pituitary gland during illumination. This induced an enhanced glucocorticoid release controlled by

adrenocorticotropic hormone (ACTH) [174]. cAMP is also essential for sperm development and motility. bPAC restored the previous disrupted fertility in transgenic mice by increasing the cAMP concentration in their sperm *in vitro* [173].

In this study, MKs expressing the photoactivated cyclases were illuminated. The results obtained showed an increase up to 700.43 nM in cAMP concentration in bPAC expressing MKs after 5 min of illumination (Figure 8). However, the concentration decreased again very quickly (Figure 9). This might be due to a high activity of PDEs in MKs. The addition of PDE 3 inhibitor cilostazol increased the cAMP concentration in illuminated MKs, but no significant difference to only light exposed cells without cilostazol treatment was detected (Figure 10). The influence of PDEs on second messenger concentrations is rather complex. Some PDEs can degrade both, cAMP and cGMP. In turn, second messengers can influence the activity of PDEs as well (1.2) [111, 113]. This is why the inhibition of PDE 3 by cilostazol might not have been adequate. Other substances or their combination need to be tested for this approach, e.g. the broad PDE inhibitor IBMX.

Besides the inhibition of PDEs, there are other possibilities to intervene with the cAMP cycle [175]. One opportunity is to use the β-adrenoreceptor agonist isoprenaline which can enhance the concentration of intracellular cAMP in combination with an inhibitor, by activating the adenylyl cyclase [176]. Another option is to reversibly induce adenylyl cyclase with forskolin [177]. However, the application is difficult due to the poor solubility of forskolin [178]. Another alternative for the experiments might be EHNA. EHNA (Erythro-9-(2-hydroxy-3-nonyl) adenine) is a specific inhibitor of PDE 2. It also inhibits the adenosine deaminase (ADA) [179]. EHNA might be a potential candidate to increase cAMP concentration in MKs because PDE 2 has an important influence on the degradation of cAMP. The use of different PDE inhibitors, their combination or the use of the formerly mentioned chemicals might be a possible starting point to improve the experiments performed.

The photoactivated guanylyl cyclase *Be*Cyclop produces cGMP after activation with light. This protein has also been tested for its applicability. Whole body

contractions of *C. elegans* were detected after illumination, due to the expression of *Be*Cyclop in body wall muscle cells of the nematode. After injection of the cyclase into *Xenopus* oocytes, the cGMP concentration increased up to 180-fold (0 to 180 µM) after 2 min of illumination with green light [107]. Furthermore, the intracellular cGMP concentration increased after the protein was expressed in Chinese hamster ovary cells and rat hippocampal neurons along with a CNG channel [180].

In MKs expressing the light-sensitive cyclase *Be*Cyclop, the cGMP concentration increased after 5 min of illumination. Values in FLC-derived MKs were higher than in BM-derived MKs (11.07 nM vs. 8.16 nM) (Figure 12; Figure 11). Dipyridamole was used to prevent the degradation of cGMP by PDE 5. The combination of PDE inhibitor and illumination produced a significantly increased cGMP level in FLC-derived MKs (11.07 nM light vs. 21.23 nM light and inhibitor) (Figure 12). To avoid PDE activity, MK membrane extract was used for one of the experiments (Figure 13) [107]. A higher cGMP concentration was reached (134 nM) compared to the results obtained with the PDE 5 inhibitor (21 nM). One explanation for the higher values could be the reduced PDE activity. Another possibility could be the longer exposure time (9 min vs. 5 min). The second messenger concentrations were determined on day 4 of FLC cultivation. Begonja *et al.* detected an increase of PDE 5 expression during MK maturation, especially on day 4 [112]. This might indicate, that PDE activity changes during the MK differentiation process and that their activity might be particularly high at the chosen time point for cGMP determination.

PDEs are present in almost every mammalian cell [181]. Therefore, application of an PDE inhibitor in a living organism is never cell-specific and might cause multiple side effects. For example, the PDE 3 inhibitor anagrelide is used to treat thrombocytosis. It inhibits megakaryopoiesis and therefore reduces the platelet count. However, the exact mechanism remains unknown. Wang *et al.* tested different PDE 3 inhibitors, especially anagrelide and its metabolites, and their impact on MK maturation. CD34 positive cells from umbilical cord blood were grown in differentiation medium, supplemented with TPO for 12 days. The test substances were added on day four. The lineage-specific marker CD61 was used as a differentiation criterion and was measured by flow cytometry on day 12.

Aside from anagrelide and trequinsin all other inhibitors (DMSO, cilostamide, cilostazol, milrinone, IBMX) did not have significant negative effects on MK maturation. The number of CD61 expressing MKs was equivalent with control cells [182].

Begonja *et al.* demonstrated that expression of proteins which are part of the signalling pathway of cAMP, increases during MK maturation. Furthermore, they showed that cGMP supports proplatelet formation [112]. Therefore, it was interesting to manipulate cAMP and cGMP concentrations in MKs with optogenetics. The results prove that the second messenger contents were increased by light (Figure 8-Figure 13). Next, it would be interesting to investigate how higher cAMP and cGMP concentrations affect MK maturation and proplatelet formation.

Next step would be to visualise the increase of cAMP and cGMP concentrations. Live-cell imaging makes it possible to observe cells in real time. Newly developed fluorophores detect the increase of cAMP or cGMP level in a cell and thus make it visible. For example, Green cGull is a single fluorescent protein based cGMP indicator. It can increase its fluorescence intensity up to 7.5-fold, compared to its initial intensity, by binding cGMP [183]. Pink Flamindo (Pink *Fl*uorescent c*AM*P *ind*icat*o*r) is a single fluorescent protein based cAMP indicator. Its fluorescence intensity can increase up to 4.2-fold, compared to its initial intensity, after binding of cAMP. This fluorophore was already tested with bPAC in HeLa cells [184]. Both binding reactions are completely reversible. The advantage of single fluorescent protein based indicators is that they only need one measurement with one wavelength for their detection [183, 184]. These fluorophores might be an interesting approach to directly visualise the raise of second messenger concentrations in MKs.

Scientific research is only just beginning to investigate the role of cAMP and cGMP in MKs. In order to better evaluate the results and to be able to intervene more specifically in MK metabolism, it is essential to better understand the significance of second messengers during this process. Furthermore, the significance of PDE isoforms in MKs needs to be examined. This would make it easier to develop a comprehensive strategy for the optimal blocking of PDEs.

4.2 Meaning of proplatelet retraction in FLC-derived MKs expressing light-sensitive ion channels and starting points for further investigations

The cation selective, light-sensitive channel ChR2 induces a depolarisation of cell membranes [152]. The construct used in this thesis, is a variant of ChR2 wildtype, called ChR2-XXL. It is characterised by a stronger expression and an extended open state. Large photocurrents were detected in *Xenopus* oocytes expressing ChR2-XXL during illumination. The construct was implemented into oocytes via cloning. Applying this construct into transgenic *Drosophila* made it possible to manipulate mono- and polysynaptic reflexes. A reversible immobilisation of larvae and the induction of the sugar sensation reaction (proboscis extension reflex) in adult animals was achieved. Furthermore, the activation of neuronal circuits, in this case, the male courtship was initiated by illumination [154].

ACRs induce hyperpolarisation of the cell membrane by selectively transporting anions. *Gt*ACR1 was tested in different cell types and organisms. By expressing this light-sensitive anion channel in neurons and cardiomyocytes with the help of a lentivirus, the silencing of neuronal activity and the manipulation of cardiomyocyte action potentials was achieved during illumination [159, 164]. Furthermore, the application into living organisms was successful. By transgenic integration of *Gt*ACR1 into the genome of zebrafish larvae, their spontaneous movement was inhibited by light [185]. Reversible inhibition of motor action and neuronal activity was detected in transgenic *Drosophila* expressing the light-sensitive anion channel [186].

The influence of ions in MK homeostasis and platelet function needs to be investigated more closely. Nevertheless, first insights have been gained in the past years. SOCE was identified as an important network of proteins and channels that regulates intra- and extracellular influx of calcium ions into cells. It is present in both MKs and platelets. Calcium is an important messenger in MKs and is involved in MK proliferation, differentiation, migration as well as in platelet production [78, 187]. Increasing calcium concentration initiates platelet activation and contributes to changes in the cytoskeleton as well as granule release [73]. Furthermore, the contribution of zinc, potassium and magnesium to MK homeostasis and platelet function has been analysed (1.1.4).

The results of the observation experiments (3.4.3) show that expression of ChR2-XXL and probably *Gt*ACR1 in FLC-derived MKs had a negative impact on proplatelet formation during illumination. MKs displayed transformations e.g. retraction of proplatelets and membrane blebbing. One possible explanation for this is that light has a phototoxic influence on the cells. However, this can be excluded since a control construct only containing the sequence for YFP was expressed in MKs and proplatelet retraction was not observed upon illumination *(personal communication)*. Therefore, the effect must be due to the impacts of the light-sensitive ion channels. It must be considered that proplatelet formation is a very dynamic process. The extension of protrusions is not continuous. According to previous studies, the elongation of proplatelets can be interrupted or even inverted [20]. It might be possible that ion influx accelerates the natural process of proplatelet formation or that ion influx has a greater influence on proplatelet retraction. Another reason for the observed retraction might be, that excessive cation or anion influx is harmful to the cells and triggers apoptosis.

The importance of apoptosis in MK homeostasis is controversially discussed. The existence of the intrinsic pathway was proven but the extrinsic pathway has not yet been investigated sufficiently [47, 188]. Several investigators postulate that locally activated caspases are necessary for proplatelet formation [189, 190]. Some believe that actin inhibition by caspases causes enhanced proplatelet formation [191]. Others support the thesis that proplatelet formation is independent of caspase activity and that MKs lose their ability to form proplatelets after the intrinsic pathway is induced [188]. All working groups detected an increased phosphatidylserine exposure on the MK surface, which among other things is a sign for apoptosis, but the exposure timepoints differed. De Botton *et al.* measured an increase in phosphatidylserine exposure on the MK surface during proplatelet formation excluding the surface of proplatelets and apoptotic MKs [189]. In contrast, Josefsson *et al.* detected an increased exposure after the completion of proplatelet formation [188]. To verify the theory about apoptosis, a determination of phosphatidylserine exposure or a staining for caspase 3 in MKs might be helpful.

Additionally, the patch clamp method could be a helpful technique to verify the actual number of ions, that is transported through the light-sensitive ion channels.

Consequently, the impact of the increasing ion concentrations could be monitored more precisely. Eventually, observations of cell behaviour may be directly related to certain ion concentrations.

Furthermore, it needs to be investigated after which time period the changes are initiated. In this study, cells were illuminated for 60 min and changes of MK morphology were observed during this time period. It needs to be verified which illumination time is necessary to detect alterations in MK behaviour or to reach a certain intracellular ion concentration. Another interesting approach would be to investigate the effects of alternating light conditions on MKs, i.e. a repetitive change between light and darkness. Eventually, a reversible change in proplatelet formation may be detected after a short exposure time and continuous observation in the dark.

The relevance of using other variants of ChR2 will be discussed in the following chapter.

4.3 Genetic modifications to improve optogenetic constructs

Genetic modification of optogenetic constructs allows the adaptation to experimental conditions. Effectiveness of e.g. light-sensitive ion channels may be increased by modifying ion selectivity, channel kinetics, light sensitivity, expression pattern and duration of the recovery period after desensitisation [192]. Additionally, efficacy can be increased by an extension of the open state and enhanced ion conductance [193]. Due to increased light sensitivity of constructs, lower light intensities are sufficient for their activation. Therefore, the risks of cell damage due to high light intensities can be reduced. Another advantage of constructs with an increased light sensitivity is that even cells in deeper layers, which express the protein, can be activated by light more easily [193].

So far, there are already many versions of ChR2 with different specifications. It might be beneficial to use them as well for long-time incubation microscopy to compare their effects on proplatelet formation. A possible starting point to optimise ChR2 is the central pore. It can be widened in order to improve ion conductance. This adjustment is, however, limited because a wider central pore increases the instability of the channel. Furthermore, when adapting the

absorption spectrum one must pay attention not to reach the wavelengths of thermal activation (630 nm) [125].

Because calcium is an important ion in platelets and MK homeostasis it would be beneficial to generate a more selective light-sensitive calcium channel for the experiments. The ChR2 mutant L132C, referred to as CatCh, has an increased ion conductance for calcium compared to the wildtype. The additional calcium ions do not originate from internal storages but from the extracellular space. This makes it possible to increase the intracellular calcium concentration by adding more calcium to the cell medium. It seems that the increased ion conductance for divalent ions also improves the sensitivity of the mutant. An explanation for this phenomenon might be the activation of voltage dependent sodium channels by membrane depolarisation due to calcium influx. It was possible to increase the calcium conductance up to 6 times and the light sensitivity up to 70-fold, compared to wildtype ChR2. The conductance of other ions remained unaltered, except for a slightly increased transport of hydrogen ions [193]. This variation of ChR2 might be an interesting candidate to investigate the effects of calcium conductance on MK homeostasis.

4.4 Improvement of exposure conditions

Some optogenetic constructs show significant dark activity. This means that transduced cells get activated without light before the actual experiment [171]. To prevent unwanted activation of the optogenetic constructs most working steps were carried out under red light (2.2.3; 2.2.4). The lamps used in this study emitted red light in the range of far red (650-720 nm). During the set up for the observation experiment, the cells were exposed to microscope light. To prevent pre-activation, a red foil was used to block light with wavelengths of <580nm. However, it cannot be excluded that the constructs ChR2-XXL and *Be*Cyclop might have been preactivated. To make sure that no pre-activation takes place before the experiment, the cells should be shielded consequently from light in the activating spectra range.

A further modified exposure may be achieved by using focused illumination on specific cell parts. This would make it possible to directly compare illuminated

and non-illuminated cell parts. Klaus Hahn *et al.* generated a photoactivated derivate of Rac1 by fusing it to a LOV domain. Thereby, the activity of the protein is blocked in the dark and is restored in the light after conformational change of the LOV domain. Rac1 is involved in the regulation of the actin cytoskeleton. By locally limited exposure, they detected polarised cell migration [194].

During the observation microscopy experiments in this thesis, the whole dish with MKs was illuminated (Figure 5). To reduce the applied light on cells, a focused illumination on specific cell parts could be beneficial. It might be possible that a restricted light application would trigger different cell reactions. For instance, a controlled induction of ion influx could cause a more specific modification of proplatelet formation instead of an apoptotic like behaviour.

4.5 Manipulation of further MK signalling pathways with optogenetic tools

Once the above described optogenetic tools, which are already available in the laboratory of our collaborator, are firmly established in MKs, one could start to manipulate other pathways which have been demonstrated to be crucial for normal platelet formation. Previous studies have shown that members of the Rho GTPase family play an important role in MK differentiation and proplatelet formation. Rho GTPases are a determining part of the cytoskeleton [195, 196]. RhoA ensures that MKs are directed to the BM sinusoids and therefore, are a checkpoint for proplatelet formation. RhoA MK-/platelet-specific deficient mice showed an impaired thrombopoiesis due to hyperpolarised MKs which enter the sinusoids more frequently [197, 198]. Mice lacking the GTPase Cdc42 also showed a dysfunctional megakaryopoiesis with reduced platelet count [195]. Optogenetic constructs of these proteins could be used to specifically manipulate their function during platelet formation.

The LOV2 Trap and Release of Protein (LOVTRAP) approach (Figure 18) enables the reversible dissociation of proteins by light. A fragment of protein A (stands as an example for a protein) is bound to the dark state of a LOV2 domain. The requested protein (POI) is coupled to the fragment of protein A. Therefore,

the requested protein is kept away from the site of action. By a light pulse, the requested protein is released and can act normal again [199].

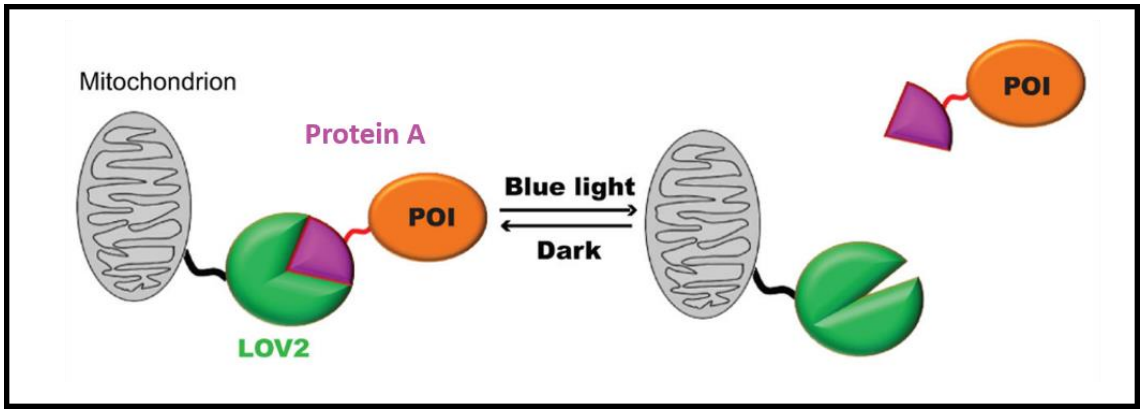

Figure 18: Schematic model of the LOVTRAP approach

Protein A is bound to the dark state of LOV2, POI is coupled to a fragment of protein A. POI is released due to blue light pulse
POI = protein of interest

Image and description taken and modified from Wang, H. et al. (2016). LOVETRAP: an optogenetic system for photoinduced protein dissociation. *Nat Methods*, 13(9), 555-758

A similar approach was applied to the Rho GTPase Rac. A LOV2 domain was coupled to Rac and blocked the active site of the protein. By a light pulse the terminal helix of the LOV2 domain was unwound and released the active site of Rac. Because Rac participates in the regulation of the cytoskeleton, selective induction of cell motility was detected. Wu *et al.* proposed to also apply this method to other Rho GTPases, e.g. Cdc42, due to their similar structure [194, 196, 200]. This may open the possibility to learn more about the significance of Cdc42 and other Rho GTPases in MK homeostasis with the help of optogenetics.

4.6 Transfer of observed results from MKs to platelets

Due to the fact that platelet production *in vitro* is very challenging (1.1.5), the generation of a genetically modified mouse line would be a possibility to get a sufficient number of platelets for research [201]. If the optogenetic construct would be expressed in MKs and platelets, the effects on platelet aggregation, thrombus formation and bleeding time could be investigated. Furthermore, one

would have the opportunity to perform experiments *in vivo*, such as two-photon microscopy studies.

ChR2 H134R induces larger conductance changes compared to the ChR2 wildtype channel. Nevertheless, the already existing mouse line which selectively expresses the ChR2 H134R mutation in MKs and platelets shows some disadvantages. High light intensities are needed for the experiments because the construct has a low sensitivity to light. A mouse model which expresses the modified ChR2-XXL (1.3.2.2) especially in MKs and platelets would be a valuable approach to study the effects on platelet function *in vitro* and *in vivo*.

4.7 Outlook and concluding remarks

The work presented here shows the establishment of optogenetic constructs in MKs for the first time. In this study, four different constructs were expressed in MKs by viral transduction. With the help of the light-sensitive cyclases, namely bPAC and *Be*Cyclop, it was possible to increase the intracellular cAMP and cGMP concentration in MKs, respectively. First data indicate that PDE activity in MKs is high. The combination of optogenetic approaches and use of inhibitors may provide new insights into the function of PDE activity as well as changes in cAMP and cGMP concentration during MK maturation and platelet production. Furthermore, retraction of proplatelets during illumination was detected in MKs, which expressed the light-sensitive ion channel, ChR2-XXL. The spreading of ChR2-XXL expressing MKs upon illumination needs to be investigated more closely in future. Additionally, it should be verified which illumination time is needed to induce these changes and what causes them. To investigate the influence of calcium on MK homeostasis it would be helpful to generate a calcium specific light-sensitive ion channel.

The use of newly generated fluorophores is a possibility to visualise the increase of second messengers in living cells. In this approach it is not necessary to treat the cells specifically to detect the increasing second messenger concentrations, but the effects of the changing exposure conditions can be visualised directly. To eliminate the impacts of pre-activation of cells before the actual experiment the exposure of cells to activating light spectra should be minimised. With an expansion of the optogenetic toolbox it would be possible to study MK signalling pathways in more detail. Finally, with a mouse line which expresses optogenetic constructs selectively in MKs and platelets it would be possible to not only analyse MKs but also platelets.

The results of this thesis may help to optimise the use of optogenetics in MKs and platelets. Further experiments using the above described or other light-sensitive proteins will lead to new insights into MK homeostasis and may help to optimise platelet production *in vitro*.

5 Bibliography

1. Spangrude, G.J., S. Heimfeld, and I.L. Weissman, *Purification and characterization of mouse hematopoietic stem cells.* Science, 1988. **241**(4861): p. 58-62.

2. Morrison, S.J. and D.T. Scadden, *The bone marrow niche for haematopoietic stem cells.* Nature, 2014. **505**(7483): p. 327-34.

3. Machlus, K.R. and J.E. Italiano, Jr., *The incredible journey: From megakaryocyte development to platelet formation.* J Cell Biol, 2013. **201**(6): p. 785-96.

4. Tober, J., et al., *The megakaryocyte lineage originates from hemangioblast precursors and is an integral component both of primitive and of definitive hematopoiesis.* Blood, 2007. **109**(4): p. 1433-41.

5. Schulze, H., *[Current models of thrombopoiesis].* Pathologe, 2010. **31 Suppl 2**: p. 183-7.

6. Avanzi, M.P. and W.B. Mitchell, *Ex vivo production of platelets from stem cells.* Br J Haematol, 2014. **165**(2): p. 237-47.

7. Arai, F. and T. Suda, *Maintenance of quiescent hematopoietic stem cells in the osteoblastic niche.* Ann N Y Acad Sci, 2007. **1106**: p. 41-53.

8. Kaushansky, K., et al., *Thrombopoietin, the Mp1 ligand, is essential for full megakaryocyte development.* Proc Natl Acad Sci U S A, 1995. **92**(8): p. 3234-8.

9. Schulze, H. and R.A. Shivdasani, *Mechanisms of thrombopoiesis.* J Thromb Haemost, 2005. **3**(8): p. 1717-24.

10. Calvi, L.M., et al., *Osteoblastic cells regulate the haematopoietic stem cell niche.* Nature, 2003. **425**(6960): p. 841-6.

11. Kopp, H.G., et al., *The bone marrow vascular niche: home of HSC differentiation and mobilization.* Physiology (Bethesda), 2005. **20**: p. 349-56.

12. Kopp, H.G., et al., *Functional heterogeneity of the bone marrow vascular niche.* Ann N Y Acad Sci, 2009. **1176**: p. 47-54.

13. Wilson, A. and A. Trumpp, *Bone-marrow haematopoietic-stem-cell niches.* Nat Rev Immunol, 2006. **6**(2): p. 93-106.

14. Battinelli, E.M., J.H. Hartwig, and J.E. Italiano, Jr., *Delivering new insight into the biology of megakaryopoiesis and thrombopoiesis.* Curr Opin Hematol, 2007. **14**(5): p. 419-26.

15. Patel, S.R., J.H. Hartwig, and J.E. Italiano, Jr., *The biogenesis of platelets from megakaryocyte proplatelets.* J Clin Invest, 2005. **115**(12): p. 3348-54.

16. Schulze, H., et al., *Characterization of the megakaryocyte demarcation membrane system and its role in thrombopoiesis.* Blood, 2006. **107**(10): p. 3868-75.

17. Behnke, O., *An electron microscope study of the megacaryocyte of the rat bone marrow. I. The development of the demarcation membrane system and the platelet surface coat.* J Ultrastruct Res, 1968. **24**(5): p. 412-33.

18. Avecilla, S.T., et al., *Chemokine-mediated interaction of hematopoietic progenitors with the bone marrow vascular niche is required for thrombopoiesis.* Nat Med, 2004. **10**(1): p. 64-71.

19. Hartwig, J. and J. Italiano, Jr., *The birth of the platelet.* J Thromb Haemost, 2003. **1**(7): p. 1580-6.

20. Bender, M., et al., *Microtubule sliding drives proplatelet elongation and is dependent on cytoplasmic dynein.* Blood, 2015. **125**(5): p. 860-8.

21. Italiano, J.E., Jr., et al., *Blood platelets are assembled principally at the ends of proplatelet processes produced by differentiated megakaryocytes.* J Cell Biol, 1999. **147**(6): p. 1299-312.

22. Diagouraga, B., et al., *Motor-driven marginal band coiling promotes cell shape change during platelet activation.* J Cell Biol, 2014. **204**(2): p. 177-85.

23. Thon, J.N., et al., *Microtubule and cortical forces determine platelet size during vascular platelet production.* Nat Commun, 2012. **3**: p. 852.

24. Thon, J.N., et al., *Cytoskeletal mechanics of proplatelet maturation and platelet release.* J Cell Biol, 2010. **191**(4): p. 861-74.

25. Junt, T., et al., *Dynamic visualization of thrombopoiesis within bone marrow.* Science, 2007. **317**(5845): p. 1767-70.

26. Kaushansky, K., *The molecular mechanisms that control thrombopoiesis.* J Clin Invest, 2005. **115**(12): p. 3339-47.

27. Krishnegowda, M. and V. Rajashekaraiah, *Platelet disorders: an overview.* Blood Coagul Fibrinolysis, 2015. **26**(5): p. 479-91.

28. Ren, Q., S. Ye, and S.W. Whiteheart, *The platelet release reaction: just when you thought platelet secretion was simple.* Curr Opin Hematol, 2008. **15**(5): p. 537-41.

29. Italiano, J.E., Jr. and R.A. Shivdasani, *Megakaryocytes and beyond: the birth of platelets*. J Thromb Haemost, 2003. **1**(6): p.

30. Savage, B., F. Almus-Jacobs, and Z.M. Ruggeri, *Specific synergy of multiple substrate-receptor interactions in platelet thrombus formation under flow.* Cell, 1998. **94**(5): p. 657-66.

31. Dutting, S., M. Bender, and B. Nieswandt, *Platelet GPVI: a target for antithrombotic therapy?!* Trends Pharmacol Sci, 2012. **33**(11): p. 583-90.

32. Ruggeri, Z.M., J.A. Dent, and E. Saldivar, *Contribution of distinct adhesive interactions to platelet aggregation in flowing blood.* Blood, 1999. **94**(1): p. 172-8.

33. Shattil, S.J. and P.J. Newman, *Integrins: dynamic scaffolds for adhesion and signaling in platelets.* Blood, 2004. **104**(6): p. 1606-15.

34. Hynes, R.O., *Integrins: bidirectional, allosteric signaling machines.* Cell, 2002. **110**(6): p. 673-87.

35. Brass, L.F., L. Zhu, and T.J. Stalker, *Minding the gaps to promote thrombus growth and stability.* J Clin Invest, 2005. **115**(12): p. 3385-92.

36. Li, Z., et al., *Signaling during platelet adhesion and activation.* Arterioscler Thromb Vasc Biol, 2010. **30**(12): p. 2341-9.

37. Varga-Szabo, D., I. Pleines, and B. Nieswandt, *Cell adhesion mechanisms in platelets.* Arterioscler Thromb Vasc Biol, 2008. **28**(3): p. 403-12.

38. Hartwig, J.H., et al., *D3 phosphoinositides and outside-in integrin signaling by glycoprotein IIb-IIIa mediate platelet actin assembly and filopodial extension induced by phorbol 12-myristate 13-acetate.* J Biol Chem, 1996. **271**(51): p. 32986-93.

39. Bearer, E.L., J.M. Prakash, and Z. Li, *Actin dynamics in platelets.* Int Rev Cytol, 2002. **217**: p. 137-82.

40. Coller, B.S. and S.J. Shattil, *The GPIIb/IIIa (integrin alphaIIbbeta3) odyssey: a technology-driven saga of a receptor with twists, turns, and even a bend.* Blood, 2008. **112**(8): p. 3011-25.

41. Andrews, R.K. and M.C. Berndt, *Platelet physiology and thrombosis.* Thromb Res, 2004. **114**(5-6): p. 447-53.

42. Anitua, E., et al., *Autologous platelets as a source of proteins for healing and tissue regeneration.* Thromb Haemost, 2004. **91**(1): p. 4-15.

43. Italiano, J.E., Jr., et al., *Angiogenesis is regulated by a novel mechanism: pro- and antiangiogenic proteins are organized into separate platelet alpha granules and differentially released.* Blood, 2008. **111**(3): p. 1227-33.

44. Gay, L.J. and B. Felding-Habermann, *Contribution of platelets to tumour metastasis.* Nat Rev Cancer, 2011. **11**(2): p. 123-34.

45. Nieswandt, B., et al., *Lysis of tumor cells by natural killer cells in mice is impeded by platelets.* Cancer Res, 1999. **59**(6): p. 1295-300.

46. Youle, R.J. and A. Strasser, *The BCL-2 protein family: opposing activities that mediate cell death.* Nat Rev Mol Cell Biol, 2008. **9**(1): p. 47-59.

47. White, M.J., et al., *Caspase-9 mediates the apoptotic death of megakaryocytes and platelets, but is dispensable for their generation and function.* Blood, 2012. **119**(18): p. 4283-90.

48. Kile, B.T., *The role of apoptosis in megakaryocytes and platelets.* Br J Haematol, 2014. **165**(2): p. 217-26.

49. Droin, N., et al., *Various functions of caspases in hematopoiesis.* Front Biosci (Landmark Ed), 2009. **14**: p. 2358-71.

50. Nagata, S., et al., *Exposure of phosphatidylserine on the cell surface.* Cell Death Differ, 2016. **23**(6): p. 952-61.

51. Segawa, K. and S. Nagata, *An Apoptotic 'Eat Me' Signal: Phosphatidylserine Exposure.* Trends Cell Biol, 2015. **25**(11): p. 639-650.

52. Zhang, H., et al., *Bcl-2 family proteins are essential for platelet survival.* Cell Death Differ, 2007. **14**(5): p. 943-51.

53. Schoenwaelder, S.M., et al., *Two distinct pathways regulate platelet phosphatidylserine exposure and procoagulant function.* Blood, 2009. **114**(3): p. 663-6.

54. Bevers, E.M., et al., *Generation of prothrombin-converting activity and the exposure of phosphatidylserine at the outer surface of platelets.* Eur J Biochem, 1982. **122**(2): p. 429-36.

55. Heemskerk, J.W., E.M. Bevers, and T. Lindhout, *Platelet activation and blood coagulation.* Thromb Haemost, 2002. **88**(2): p. 186-93.

56. Tolhurst, G., et al., *Interplay between P2Y(1), P2Y(12), and P2X(1) receptors in the activation of megakaryocyte cation influx currents by ADP: evidence that the primary megakaryocyte represents a fully functional model of platelet P2 receptor signaling.* Blood, 2005. **106**(5): p. 1644-51.

57. Mahaut-Smith, M.P., *The unique contribution of ion channels to platelet and megakaryocyte function.* J Thromb Haemost, 2012. **10**(9): p. 1722-32.

58. Neher, E., B. Sakmann, and J.H. Steinbach, *The extracellular patch clamp: a method for resolving currents through individual open channels in biological membranes.* Pflugers Arch, 1978. **375**(2): p. 219-28.

59. Carter, R.N., et al., *Molecular and electrophysiological characterization of transient receptor potential ion channels in the primary murine megakaryocyte.* J Physiol, 2006. **576**(Pt 1): p. 151-62.

60. Heyns Adu, P., et al., *Zinc-induced platelet aggregation is mediated by the fibrinogen receptor and is not accompanied by release or by thromboxane synthesis.* Blood, 1985. **66**(1): p. 213-9.

61. Taylor, K.A. and N. Pugh, *The contribution of zinc to platelet behaviour during haemostasis and thrombosis.* Metallomics, 2016. **8**(2): p. 144-55.

62. Watson, B.R., et al., *Zinc is a transmembrane agonist that induces platelet activation in a tyrosine phosphorylation-dependent manner.* Metallomics, 2016. **8**(1): p. 91-100.

63. Mammadova-Bach, E. and A. Braun, *Zinc Homeostasis in Platelet-Related Diseases.* Int J Mol Sci, 2019. **20**(21).

64. McCloskey, C., et al., *Kv1.3 is the exclusive voltage-gated K+ channel of platelets and megakaryocytes: roles in membrane potential, Ca2+ signalling and platelet count.* J Physiol, 2010. **588**(Pt 9): p. 1399-406.

65. Stritt, S., et al., *Defects in TRPM7 channel function deregulate thrombopoiesis through altered cellular Mg(2+) homeostasis and cytoskeletal architecture.* Nat Commun, 2016. **7**: p. 11097.

66. Hathaway, D.R. and R.S. Adelstein, *Human platelet myosin light chain kinase requires the calcium-binding protein calmodulin for activity.* Proc Natl Acad Sci U S A, 1979. **76**(4): p. 1653-7.

67. Mahaut-Smith, M.P., S. Jones, and R.J. Evans, *The P2X1 receptor and platelet function.* Purinergic Signal, 2011. **7**(3): p. 341-56.

68. Yeromin, A.V., et al., *Molecular identification of the CRAC channel by altered ion selectivity in a mutant of Orai.* Nature, 2006. **443**(7108): p. 226-9.

69. Prakriya, M., et al., *Orai1 is an essential pore subunit of the CRAC channel.* Nature, 2006. **443**(7108): p. 230-3.

70. Liou, J., et al., *STIM is a Ca2+ sensor essential for Ca2+-store-depletion-triggered Ca2+ influx.* Curr Biol, 2005. **15**(13): p. 1235-41.

71. Cahalan, M.D., *STIMulating store-operated Ca(2+) entry.* Nat Cell Biol, 2009. **11**(6): p. 669-77.

72. Varga-Szabo, D., A. Braun, and B. Nieswandt, *STIM and Orai in platelet function.* Cell Calcium, 2011. **50**(3): p. 270-8.

73. Varga-Szabo, D., A. Braun, and B. Nieswandt, *Calcium signaling in platelets.* J Thromb Haemost, 2009. **7**(7): p. 1057-66.

74. Grosse, J., et al., *An EF hand mutation in Stim1 causes premature platelet activation and bleeding in mice.* J Clin Invest, 2007. **117**(11): p. 3540-50.

75. Braun, A., et al., *Orai1 (CRACM1) is the platelet SOC channel and essential for pathological thrombus formation.* Blood, 2009. **113**(9): p. 2056-63.

76. van Kruchten, R., et al., *Antithrombotic potential of blockers of store-operated calcium channels in platelets.* Arterioscler Thromb Vasc Biol, 2012. **32**(7): p. 1717-23.

77. Gilio, K., et al., *Roles of platelet STIM1 and Orai1 in glycoprotein VI- and thrombin-dependent procoagulant activity and thrombus formation.* J Biol Chem, 2010. **285**(31): p. 23629-38.

78. Di Buduo, C.A., et al., *The importance of calcium in the regulation of megakaryocyte function.* Haematologica, 2014. **99**(4): p. 769-78.

79. Di Buduo, C.A., et al., *Defective interaction of mutant calreticulin and SOCE in megakaryocytes from patients with myeloproliferative neoplasms.* Blood, 2020. **135**(2): p. 133-144.

80. Somasundaram, B. and M.P. Mahaut-Smith, *Three cation influx currents activated by purinergic receptor stimulation in rat megakaryocytes.* J Physiol, 1994. **480 (Pt 2)**: p. 225-31.

81. Somasundaram, B. and M.P. Mahaut-Smith, *A novel monovalent cation channel activated by inositol trisphosphate in the plasma membrane of rat megakaryocytes.* J Biol Chem, 1995. **270**(28): p. 16638-44.

82. Hussain, J.F. and M.P. Mahaut-Smith, *ADP and inositol trisphosphate evoke oscillations of a monovalent cation conductance in rat megakaryocytes.* J Physiol, 1998. **511 (Pt 3)**: p. 791-801.

83. Stasi, R., *How to approach thrombocytopenia.* Hematology Am Soc Hematol Educ Program, 2012. **2012**: p. 191-7.

84. Sullivan, M.T., et al., *Blood collection and transfusion in the United States in 2001.* Transfusion, 2007. **47**(3): p. 385-94.

85. Cardigan, R. and L.M. Williamson, *The quality of platelets after storage for 7 days.* Transfus Med, 2003. **13**(4): p. 173-87.

86. Dunois-Larde, C., et al., *Exposure of human megakaryocytes to high shear rates accelerates platelet production.* Blood, 2009. **114**(9): p. 1875-83.

87. de Sauvage, F.J., et al., *Physiological regulation of early and late stages of megakaryocytopoiesis by thrombopoietin.* J Exp Med, 1996. **183**(2): p. 651-6.

88. de Sauvage, F.J., et al., *Stimulation of megakaryocytopoiesis and thrombopoiesis by the c-Mpl ligand.* Nature, 1994. **369**(6481): p. 533-8.

89. Bartley, T.D., et al., *Identification and cloning of a megakaryocyte growth and development factor that is a ligand for the cytokine receptor Mpl.* Cell, 1994. **77**(7): p. 1117-24.

90. Lok, S., et al., *Cloning and expression of murine thrombopoietin cDNA and stimulation of platelet production in vivo.* Nature, 1994. **369**(6481): p. 565-8.

91. Sohma, Y., et al., *Molecular cloning and chromosomal localization of the human thrombopoietin gene.* FEBS Lett, 1994. **353**(1): p. 57-61.

92. Kaushansky, K., *Physiology and preclinical studies of thrombopoietin.* Curr Opin Hematol, 1995. **2**(3): p. 172-6.

93. Deutsch, V.R. and A. Tomer, *Advances in megakaryocytopoiesis and thrombopoiesis: from bench to bedside.* Br J Haematol, 2013. **161**(6): p. 778-93.

94. Eckly, A., et al., *Biogenesis of the demarcation membrane system (DMS) in megakaryocytes.* Blood, 2014. **123**(6): p. 921-30.

95. Kaushansky, K., et al., *Promotion of megakaryocyte progenitor expansion and differentiation by the c-Mpl ligand thrombopoietin.* Nature, 1994. **369**(6481): p. 568-71.

96. Matsunaga, T., et al., *Ex vivo large-scale generation of human platelets from cord blood CD34+ cells.* Stem Cells, 2006. **24**(12): p. 2877-87.

97. Takayama, N. and K. Eto, *Pluripotent stem cells reveal the developmental biology of human megakaryocytes and provide a source of platelets for clinical application.* Cell Mol Life Sci, 2012. **69**(20): p. 3419-28.

98. Takayama, N., et al., *Transient activation of c-MYC expression is critical for efficient platelet generation from human induced pluripotent stem cells.* J Exp Med, 2010. **207**(13): p. 2817-30.

99. Sullenbarger, B., et al., *Prolonged continuous in vitro human platelet production using three-dimensional scaffolds.* Exp Hematol, 2009. **37**(1): p. 101-10.

100. Pallotta, I., et al., *Three-dimensional system for the in vitro study of megakaryocytes and functional platelet production using silk-based vascular tubes.* Tissue Eng Part C Methods, 2011. **17**(12): p. 1223-32.

101. Torisawa, Y.S., et al., *Bone marrow-on-a-chip replicates hematopoietic niche physiology in vitro.* Nat Methods, 2014. **11**(6): p. 663-9.

102. Thon, J.N., et al., *Platelet bioreactor-on-a-chip.* Blood, 2014. **124**(12): p. 1857-67.

103. Shemarova, I.V., *cAMP-dependent signal pathways in unicellular eukaryotes.* Crit Rev Microbiol, 2009. **35**(1): p. 23-42.

104. Gancedo, J.M., *Biological roles of cAMP: variations on a theme in the different kingdoms of life.* Biological Reviews, 2013. **88**(3): p. 645-668.

105. Kobayashi, M., J. Buck, and L.R. Levin, *Conservation of functional domain structure in bicarbonate-regulated "soluble" adenylyl cyclases in bacteria and eukaryotes.* Dev Genes Evol, 2004. **214**(10): p. 503-9.

106. Richter, W., *3',5' Cyclic nucleotide phosphodiesterases class III: members, structure, and catalytic mechanism.* Proteins, 2002. **46**(3): p. 278-86.

107. Gao, S., et al., *Optogenetic manipulation of cGMP in cells and animals by the tightly light-regulated guanylyl-cyclase opsin CyclOp.* Nat Commun, 2015. **6**: p. 8046.

108. Lucas, K.A., et al., *Guanylyl cyclases and signaling by cyclic GMP.* Pharmacol Rev, 2000. **52**(3): p. 375-414.

109. Liu, Y., et al., *Cilostazol (pletal): a dual inhibitor of cyclic nucleotide phosphodiesterase type 3 and adenosine uptake.* Cardiovasc Drug Rev, 2001. **19**(4): p. 369-86.

110. Zoraghi, R., et al., *Structural and functional features in human PDE5A1 regulatory domain that provide for allosteric cGMP binding, dimerization, and regulation.* J Biol Chem, 2005. **280**(12): p. 12051-63.

111. Bender, A.T. and J.A. Beavo, *Cyclic nucleotide phosphodiesterases: molecular regulation to clinical use.* Pharmacol Rev, 2006. **58**(3): p. 488-520.

112. Begonja, A.J., et al., *Differential roles of cAMP and cGMP in megakaryocyte maturation and platelet biogenesis.* Exp Hematol, 2013. **41**(1): p. 91-101 e4.

113. Dickinson, N.T., E.K. Jang, and R.J. Haslam, *Activation of cGMP-stimulated phosphodiesterase by nitroprusside limits cAMP accumulation in human platelets: effects on platelet aggregation.* Biochem J, 1997. **323 (Pt 2)**: p. 371-7.

114. Rondina, M.T. and A.S. Weyrich, *Targeting phosphodiesterases in anti-platelet therapy.* Handb Exp Pharmacol, 2012(210): p. 225-38.

115. Shakur, Y., et al., *Regulation and function of the cyclic nucleotide phosphodiesterase (PDE3) gene family.* Prog Nucleic Acid Res Mol Biol, 2001. **66**: p. 241-77.

116. Gresele, P., S. Momi, and E. Falcinelli, *Anti-platelet therapy: phosphodiesterase inhibitors.* Br J Clin Pharmacol, 2011. **72**(4): p. 634-46.

117. Schrör, K., *The pharmacology of cilostazol.* Diabetes Obes Metab, 2002. **4 Suppl 2**: p. S14-9.

118. Klabunde, R.E., *Dipyridamole inhibition of adenosine metabolism in human blood.* Eur J Pharmacol, 1983. **93**(1-2): p. 21-6.

119. Neri Serneri, G.G., et al., *Enhanced prostacyclin production by dipyridamole in man.* Eur J Clin Pharmacol, 1981. **21**(1): p. 9-15.

120. Deisseroth, K., *Optogenetics.* Nat Methods, 2011. **8**(1): p. 26-9.

121. Zhang, F., et al., *Channelrhodopsin-2 and optical control of excitable cells.* Nat Methods, 2006. **3**(10): p. 785-92.

122. Oesterhelt, D. and W. Stoeckenius, *Rhodopsin-like protein from the purple membrane of Halobacterium halobium.* Nat New Biol, 1971. **233**(39): p. 149-52.

123. Oesterhelt, D. and W. Stoeckenius, *Functions of a new photoreceptor membrane.* Proc Natl Acad Sci U S A, 1973. **70**(10): p. 2853-7.

124. Deisseroth, K., *Optogenetics: 10 years of microbial opsins in neuroscience.* Nat Neurosci, 2015. **18**(9): p. 1213-25.

125. Grote, M., M. Engelhard, and P. Hegemann, *Of ion pumps, sensors and channels - perspectives on microbial rhodopsins between science and history.* Biochim Biophys Acta, 2014. **1837**(5): p. 533-45.

126. Hildebrand, E. and N. Dencher, *Two photosystems controlling behavioural responses of Halobacterium halobium.* Nature, 1975. **257**(5521): p. 46-8.

127. Matsuno-Yagi, A. and Y. Mukohata, *Two possible roles of bacteriorhodopsin; a comparative study of strains of Halobacterium halobium differing in pigmentation.* Biochem Biophys Res Commun, 1977. **78**(1): p. 237-43.

128. Schobert, B. and J.K. Lanyi, *Halorhodopsin is a light-driven chloride pump.* J Biol Chem, 1982. **257**(17): p. 10306-13.

129. Zhang, F., et al., *Circuit-breakers: optical technologies for probing neural signals and systems.* Nat Rev Neurosci, 2007. **8**(8): p. 577-81.

130. Han, X. and E.S. Boyden, *Multiple-color optical activation, silencing, and desynchronization of neural activity, with single-spike temporal resolution.* PLoS One, 2007. **2**(3): p. e299.

131. Berndt, A. and K. Deisseroth, *OPTOGENETICS. Expanding the optogenetics toolkit.* Science, 2015. **349**(6248): p. 590-1.

132. Sineshchekov, O.A., K.H. Jung, and J.L. Spudich, *Two rhodopsins mediate phototaxis to low- and high-intensity light in Chlamydomonas reinhardtii.* Proc Natl Acad Sci U S A, 2002. **99**(13): p. 8689-94.

133. Sasaki, J. and J.L. Spudich, *Proton transport by sensory rhodopsins and its modulation by transducer-binding.* Biochim Biophys Acta, 2000. **1460**(1): p. 230-9.

134. Schlesner, M., et al., *The protein interaction network of a taxis signal transduction system in a halophilic archaeon.* BMC Microbiol, 2012. **12**: p. 272.

135. Nagel, G., et al., *Channelrhodopsin-1: a light-gated proton channel in green algae.* Science, 2002. **296**(5577): p. 2395-8.

136. Ehlenbeck, S., et al., *Evidence for a light-induced H(+) conductance in the eye of the green alga Chlamydomonas reinhardtii.* Biophys J, 2002. **82**(2): p. 740-51.

137. Nagel, G., et al., *Channelrhodopsins: directly light-gated cation channels.* Biochem Soc Trans, 2005. **33**(Pt 4): p. 863-6.

138. Bamann, C., G. Nagel, and E. Bamberg, *Microbial rhodopsins in the spotlight.* Curr Opin Neurobiol, 2010. **20**(5): p. 610-6.

139. Nagel, G., et al., *Light activation of channelrhodopsin-2 in excitable cells of Caenorhabditis elegans triggers rapid behavioral responses.* Curr Biol, 2005. **15**(24): p. 2279-84.

140. Boyden, E.S., et al., *Millisecond-timescale, genetically targeted optical control of neural activity.* Nat Neurosci, 2005. **8**(9): p. 1263-8.

141. Bi, A., et al., *Ectopic expression of a microbial-type rhodopsin restores visual responses in mice with photoreceptor degeneration.* Neuron, 2006. **50**(1): p. 23-33.

142. Aravanis, A.M., et al., *An optical neural interface: in vivo control of rodent motor cortex with integrated fiberoptic and optogenetic technology.* J Neural Eng, 2007. **4**(3): p. S143-56.

143. Arenkiel, B.R., et al., *In vivo light-induced activation of neural circuitry in transgenic mice expressing channelrhodopsin-2.* Neuron, 2007. **54**(2): p. 205-18.

144. Zhang, F., et al., *Multimodal fast optical interrogation of neural circuitry.* Nature, 2007. **446**(7136): p. 633-9.

145. Kushibiki, T., et al., *Optogenetic control of insulin secretion by pancreatic beta-cells in vitro and in vivo.* Gene Ther, 2015. **22**(7): p. 553-9.

146. Bruegmann, T., et al., *Optogenetic control of heart muscle in vitro and in vivo.* Nat Methods, 2010. **7**(11): p. 897-900.

147. Nussinovitch, U. and L. Gepstein, *Optogenetics for in vivo cardiac pacing and resynchronization therapies.* Nat Biotechnol, 2015. **33**(7): p. 750-4.

148. Bamann, C., et al., *Spectral characteristics of the photocycle of channelrhodopsin-2 and its implication for channel function.* J Mol Biol, 2008. **375**(3): p. 686-94.

149. Yizhar, O., et al., *Microbial opsins: a family of single-component tools for optical control of neural activity.* Cold Spring Harb Protoc, 2011. **2011**(3): p. top102.

150. Zhang, F., et al., *The microbial opsin family of optogenetic tools.* Cell, 2011. **147**(7): p. 1446-57.

151. Ernst, O.P., et al., *Microbial and animal rhodopsins: structures, functions, and molecular mechanisms.* Chem Rev, 2014. **114**(1): p. 126-63.

152. Nagel, G., et al., *Channelrhodopsin-2, a directly light-gated cation-selective membrane channel.* Proc Natl Acad Sci U S A, 2003. **100**(24): p. 13940-5.

153. Hegemann, P., S. Ehlenbeck, and D. Gradmann, *Multiple photocycles of channelrhodopsin.* Biophys J, 2005. **89**(6): p. 3911-8.

154. Dawydow, A., et al., *Channelrhodopsin-2-XXL, a powerful optogenetic tool for low-light applications.* Proc Natl Acad Sci U S A, 2014. **111**(38): p. 13972-7.

155. Scholz, F., et al., *Tuning the primary reaction of channelrhodopsin-2 by imidazole, pH, and site-specific mutations.* Biophys J, 2012. **102**(11): p. 2649-57.

156. Chow, B.Y., et al., *High-performance genetically targetable optical neural silencing by light-driven proton pumps.* Nature, 2010. **463**(7277): p. 98-102.

157. Wietek, J., et al., *Conversion of channelrhodopsin into a light-gated chloride channel.* Science, 2014. **344**(6182): p. 409-12.

158. Berndt, A., et al., *Structure-guided transformation of channelrhodopsin into a light-activated chloride channel.* Science, 2014. **344**(6182): p. 420-4.

159. Govorunova, E.G., et al., *NEUROSCIENCE. Natural light-gated anion channels: A family of microbial rhodopsins for advanced optogenetics.* Science, 2015. **349**(6248): p. 647-50.

160. Mahn, M., et al., *High-efficiency optogenetic silencing with soma-targeted anion-conducting channelrhodopsins.* Nat Commun, 2018. **9**(1): p. 4125.

161. Han, X., *In vivo application of optogenetics for neural circuit analysis.* ACS Chem Neurosci, 2012. **3**(8): p. 577-84.

162. Govorunova, E.G., et al., *Extending the Time Domain of Neuronal Silencing with Cryptophyte Anion Channelrhodopsins.* eNeuro, 2018. **5**(3).

163. Govorunova, E.G., et al., *The Expanding Family of Natural Anion Channelrhodopsins Reveals Large Variations in Kinetics, Conductance, and Spectral Sensitivity.* Sci Rep, 2017. **7**: p. 43358.

164. Govorunova, E.G., et al., *Anion channelrhodopsins for inhibitory cardiac optogenetics.* Sci Rep, 2016. **6**: p. 33530.

165. Iseki, M., et al., *A blue-light-activated adenylyl cyclase mediates photoavoidance in Euglena gracilis.* Nature, 2002. **415**(6875): p. 1047-51.

166. Raffelberg, S., et al., *A LOV-domain-mediated blue-light-activated adenylate (adenylyl) cyclase from the cyanobacterium Microcoleus chthonoplastes PCC 7420.* Biochem J, 2013. **455**(3): p. 359-65.

167. Weber, S., *Light-driven enzymatic catalysis of DNA repair: a review of recent biophysical studies on photolyase.* Biochim Biophys Acta, 2005. **1707**(1): p. 1-23.

168. Yoshikawa, S., et al., *Kinetic analysis of the activation of photoactivated adenylyl cyclase (PAC), a blue-light receptor for photomovements of Euglena.* Photochem Photobiol Sci, 2005. **4**(9): p. 727-31.

169. Gomelsky, M. and G. Klug, *BLUF: a novel FAD-binding domain involved in sensory transduction in microorganisms.* Trends Biochem Sci, 2002. **27**(10): p. 497-500.

170. Ryu, M.H., et al., *Natural and engineered photoactivated nucleotidyl cyclases for optogenetic applications.* J Biol Chem, 2010. **285**(53): p. 41501-8.

171. Stierl, M., et al., *Light modulation of cellular cAMP by a small bacterial photoactivated adenylyl cyclase, bPAC, of the soil bacterium Beggiatoa.* J Biol Chem, 2011. **286**(2): p. 1181-8.

172. Avelar, G.M., et al., *A rhodopsin-guanylyl cyclase gene fusion functions in visual perception in a fungus.* Curr Biol, 2014. **24**(11): p. 1234-40.

173. Jansen, V., et al., *Controlling fertilization and cAMP signaling in sperm by optogenetics.* Elife, 2015. **4**.

174. De Marco, R.J., et al., *Optogenetic elevation of endogenous glucocorticoid level in larval zebrafish.* Front Neural Circuits, 2013. **7**: p. 82.

175. Komas, N., C. Lugnier, and J.C. Stoclet, *Endothelium-dependent and independent relaxation of the rat aorta by cyclic nucleotide phosphodiesterase inhibitors.* Br J Pharmacol, 1991. **104**(2): p. 495-503.

176. Maurice, D.H. and R.J. Haslam, *Nitroprusside enhances isoprenaline-induced increases in cAMP in rat aortic smooth muscle.* Eur J Pharmacol, 1990. **191**(3): p. 471-5.

177. Seamon, K.B., W. Padgett, and J.W. Daly, *Forskolin: unique diterpene activator of adenylate cyclase in membranes and in intact cells.* Proc Natl Acad Sci U S A, 1981. **78**(6): p. 3363-7.

178. Sengupta, S. and G. Mehta, *Natural products as modulators of the cyclic-AMP pathway: evaluation and synthesis of lead compounds.* Org Biomol Chem, 2018. **16**(35): p. 6372-6390.

179. Podzuweit, T., P. Nennstiel, and A. Muller, *Isozyme selective inhibition of cGMP-stimulated cyclic nucleotide phosphodiesterases by erythro-9-(2-hydroxy-3-nonyl) adenine.* Cell Signal, 1995. **7**(7): p. 733-8.

180. Scheib, U., et al., *The rhodopsin-guanylyl cyclase of the aquatic fungus Blastocladiella emersonii enables fast optical control of cGMP signaling.* Sci Signal, 2015. **8**(389): p. rs8.

181. Reinhardt, R.R., et al., *Distinctive anatomical patterns of gene expression for cGMP-inhibited cyclic nucleotide phosphodiesterases.* J Clin Invest, 1995. **95**(4): p. 1528-38.

182. Wang, G., et al., *Comparison of the biological activities of anagrelide and its major metabolites in haematopoietic cell cultures.* Br J Pharmacol, 2005. **146**(3): p. 324-32.

183. Matsuda, S., et al., *Generation of a cGMP Indicator with an Expanded Dynamic Range by Optimization of Amino Acid Linkers between a Fluorescent Protein and PDE5alpha.* ACS Sens, 2017. **2**(1): p. 46-51.

184. Harada, K., et al., *Red fluorescent protein-based cAMP indicator applicable to optogenetics and in vivo imaging.* Sci Rep, 2017. **7**(1): p. 7351.

185. Mohamed, G.A., et al., *Optical inhibition of larval zebrafish behaviour with anion channelrhodopsins.* BMC Biol, 2017. **15**(1): p. 103.

186. Mohammad, F., et al., *Optogenetic inhibition of behavior with anion channelrhodopsins.* Nat Methods, 2017. **14**(3): p. 271-274.

187. Di Buduo, C.A., A. Balduini, and F. Moccia, *Pathophysiological Significance of Store-Operated Calcium Entry in Megakaryocyte Function: Opening New Paths for Understanding the Role of Calcium in Thrombopoiesis.* Int J Mol Sci, 2016. **17**(12).

188. Josefsson, E.C., et al., *Megakaryocytes possess a functional intrinsic apoptosis pathway that must be restrained to survive and produce platelets.* J Exp Med, 2011. **208**(10): p. 2017-31.

189. De Botton, S., et al., *Platelet formation is the consequence of caspase activation within megakaryocytes.* Blood, 2002. **100**(4): p. 1310-7.

190. Clarke, M.C., et al., *Compartmentalized megakaryocyte death generates functional platelets committed to caspase-independent death.* J Cell Biol, 2003. **160**(4): p. 577-87.

191. Avanzi, M.P., et al., *Actin inhibition increases megakaryocyte proplatelet formation through an apoptosis-dependent mechanism.* PLoS One, 2015. **10**(4): p. e0125057.

192. Knopfel, T., et al., *Toward the second generation of optogenetic tools.* J Neurosci, 2010. **30**(45): p. 14998-5004.

193. Kleinlogel, S., et al., *Ultra light-sensitive and fast neuronal activation with the Ca(2)+-permeable channelrhodopsin CatCh.* Nat Neurosci, 2011. **14**(4): p. 513-8.

194. Wu, Y.I., et al., *A genetically encoded photoactivatable Rac controls the motility of living cells.* Nature, 2009. **461**(7260): p. 104-8.

195. Pleines, I., et al., *Multiple alterations of platelet functions dominated by increased secretion in mice lacking Cdc42 in platelets.* Blood, 2010. **115**(16): p. 3364-73.

196. Nobes, C.D. and A. Hall, *Rho, rac, and cdc42 GTPases regulate the assembly of multimolecular focal complexes associated with actin stress fibers, lamellipodia, and filopodia.* Cell, 1995. **81**(1): p. 53-62.

197. Dutting, S., et al., *A Cdc42/RhoA regulatory circuit downstream of glycoprotein Ib guides transendothelial platelet biogenesis.* Nat Commun, 2017. **8**: p. 15838.

198. Pleines, I., et al., *Megakaryocyte-specific RhoA deficiency causes macrothrombocytopenia and defective platelet activation in hemostasis and thrombosis.* Blood, 2012. **119**(4): p. 1054-63.

199. Wang, H., et al., *LOVTRAP: an optogenetic system for photoinduced protein dissociation.* Nat Methods, 2016. **13**(9): p. 755-8.

200. Harper, S.M., L.C. Neil, and K.H. Gardner, *Structural basis of a phototropin light switch.* Science, 2003. **301**(5639): p. 1541-4.

201. Pendaries, C., S.P. Watson, and J.C. Spalton, *Methods for genetic modification of megakaryocytes and platelets.* Platelets, 2007. **18**(6): p. 393-408.

6 List of figures

7 List of tables

8 Appendix

8.1 Abbreviations

Abbreviation	Prolongation
ACR	anion channel rhodopsin
ACTH	adrenocorticotropic hormone
ADA	adenosine deaminase
ADP	adenosine diphosphate
Arch	archaerhodopsin
ATP	adenosine triphosphate
***Be*Cyclop**	cyclase opsin from *Blastocladiella emersonii*
BLUF	blue light using FAD
BM	bone marrow
bPAC	bacterial photoactivated adenylyl cyclase
BR	bacteriorhodopsin
BSA	bovine serum albumin
cAMP	cyclic adenosine monophosphate
cGMP	cyclic guanosine monophosphate
chop	channelopsin
ChR	channelrhodopsin
CNG	cyclic nucleotide gated
CRAC	calcium release activated calcium
DMS	demarcation membrane system
DMSO	dimethyl sulfoxide
DTT	dithiothreitol
ECM	extracellular matrix
EHNA	erythro-9-(2-hydroxy-3-nonyl) adenine)
euPAC	photoactivated adenylyl cyclase from *Euglenia gracilis*
FAD	flavin adenine dinucleotide
FCS	foetal calf serum
FLC	foetal liver cells
GPCR	g-protein coupled receptor
***Gt*ACR1**	anion channel rhodopsin from *Guillardia theta*
GTP	guanosine triphosphate
Halo/NpHR	halorhodopsin
HEK	human embryonic kidney cells
HR	halorhodopsin
HSC	heamatopoietic stem cells
Htr	halobacterial transducer

IMS	invaginated membrane system
IP3	inositol triphosphate
iPSC	induced pluripotent stem cells
ITAM	immunoreceptor tyrosine-based activation motif
LOV	light oxygen voltage
MK	megakaryocyte
ONI	optical neural interface
PBS	phosphate buffered saline
PDE	phosphodiesterase
PEI	polyethyleneimine
Pen/Strep	Penicillin/Streptomycin
PFA	paraformaldehyde
PKA	protein kinase A
PKG	protein kinase G
SCF	stem cell factor
SR	sensory rhodopsins
STIM1	stromal interaction molecule 1
TPO	thrombopoietin
vWF	von-Willebrand-Factor
YFP	yellow fluorescent protein

8.2 Acknowledgements

I would like to acknowledge the following persons without whom this thesis could not have been completed. I want to thank…

- my supervisor Dr. Markus Bender who gave me the opportunity to work on this project. He provided constant support and guidance during my whole work.
- Prof. Dr. Georg Nagel and Prof. Dr. Alma Zernecke-Madsen for their contribution as members of my thesis committee and their valuable feedback during committee meetings.
- Prof. Dr. Georg Nagel and his working group, especially Dr. Shiqiang Gao for providing all optogenetic constructs for the experiments and performing the measurements of the second messengers cAMP and cGMP.
- Yvonne and Markus who showed me the initially so unfamiliar world of the laboratory and patiently answered countless questions. Additionally, Markus helped me considerably with the microscopic images of the construct expression (Figure 6; Figure 7).
- Ruth and Lucy for helping me not to lose my courage even in case of setbacks and to finally complete the tasks. Furthermore, they were a great help for proofreading.
- my parents, who gave me the opportunity to concentrate exclusively on my thesis and supported me at every step of my education. For this I´m more than grateful.
- Paul, who accompanied me through all highs and lows of the project. I wouldn´t be where I am without you.

8.3 Curriculum vitae

8.4 Affidavit

I hereby confirm that my thesis entitled “Regulation of ion conductance and cAMP/cGMP concentration in megakaryocytes by light” is the result of my own work. I did not receive any help or support from commercial consultants. All sources and/or materials applied are listed and specified in the thesis.

Furthermore, I confirm that this thesis has not yet been submitted as part of another examination process neither in identical nor in similar form.

Würzburg, July 2020 _____

8.5 Eidesstaatliche Erklärung

Hiermit erkläre ich an Eides statt, die Dissertation „Regulation der Ionenleitfähigkeit und cAMP/cGMP Konzentration in Megakaryozyten durch Licht“ eigenständig, das heißt insbesondere selbstständig und ohne Hilfe eines kommerziellen Promotionsberaters, angefertigt und keine anderen als die von mir angegebenen Quellen und Hilfsmittel verwendet zu haben.

Ich erkläre außerdem, dass die Dissertation weder in gleicher noch in ähnlicher Form bereits in einem anderen Prüfungsverfahren vorgelegen hat.

Würzburg, July 2020 _____